AD_____

Award Number: DAMD17-00-1-0040

TITLE: An Embryonic Growth Pathway is Reactivated in Human Prostate Cancer

PRINCIPAL INVESTIGATOR: Wade Bushman, M.D., Ph.D.

CONTRACTING ORGANIZATION: University of Wisconsin
Madison, WI 53706

REPORT DATE: June 2005

TYPE OF REPORT: Final

PREPARED FOR: U.S. Army Medical Research and Materiel Command
Fort Detrick, Maryland 21702-5012

DISTRIBUTION STATEMENT: Approved for Public Release;
Distribution Unlimited

REPORT DOCUMENTATION PAGE

Form Approved
OMB No. 0704-0188

1. REPORT DATE *(DD-MM-YYYY)*	2. REPORT TYPE	3. DATES COVERED *(From - To)*
01-06-2005	Final	15 Jan 2000 - 31 May 2005

4. TITLE AND SUBTITLE

An Embryonic Growth Pathway is Reactivated in Human Prostate Cancer

5a. CONTRACT NUMBER

5b. GRANT NUMBER
DAMD17-00-1-0040

5c. PROGRAM ELEMENT NUMBER

6. AUTHOR(S)

Wade Bushman, M.D., Ph.D.

5d. PROJECT NUMBER

5e. TASK NUMBER

5f. WORK UNIT NUMBER

7. PERFORMING ORGANIZATION NAME(S) AND ADDRESS(ES)

University of Wisconsin
Madison, WI 53706

8. PERFORMING ORGANIZATION REPORT NUMBER

9. SPONSORING / MONITORING AGENCY NAME(S) AND ADDRESS(ES)
U.S. Army Medical Research and Materiel Command
Fort Detrick, Maryland 21702-5012

10. SPONSOR/MONITOR'S ACRONYM(S)

11. SPONSOR/MONITOR'S REPORT NUMBER(S)

12. DISTRIBUTION / AVAILABILITY STATEMENT
Approved for Public Release; Distribution Unlimited

13. SUPPLEMENTARY NOTES

14. ABSTRACT

Epithelial-mesenchymal interactions in prostate cancer represent a promising target for drug therapies to arrest or slow tumor growth. For this potential to be realized, it is necessary to identify one specific epithelial-mesenchymal interaction which is critical for tumor growth. We have shown that *Sonic hedgehog* (*Shh*) signaling pathway is absolutely required for normal prostate development. Our preliminary studies show this pathway is expressed at very low levels in the normal adult prostate but reactivated in human prostate cancer. This research postulates that prostate cancer cells commandeer this normal epithelial-mesenchymal signaling pathway to recruit stromal cells to support abnormal tumor growth and tests the hypothesis that Shh signaling promotes prostate tumor growth. The primary goal of the study is to establish the concept that prostate tumor growth is promoted by re-activation of the Shh-Gli pathway and identify this as a novel target for drug treatment to slow or arrest prostate cancer growth.

15. SUBJECT TERMS
Prostate cancer, Sonic Hedgehog

16. SECURITY CLASSIFICATION OF:			17. LIMITATION OF ABSTRACT	18. NUMBER OF PAGES	19a. NAME OF RESPONSIBLE PERSON
a. REPORT	b. ABSTRACT	c. THIS PAGE			19b. TELEPHONE NUMBER *(include area code)*
U	U	U	UU	21	

Table of Contents

Introduction:

This funded project addresses the role of hedgehog signaling in prostate cancer. Using a well characterized xenograft model, the purpose of the proposal is to characterize sonic hedgehog (Shh) expression in human prostate cancer, to examine the affect of Shh overexpression on prostate xenograft tumor growth, and to determine the effect of Shh loss of function on tumor growth.

Body:

The research goals in the statement of work were addressed as planned. Specifically, the goals 1a, 1c, 2a, 2b, and 2d were accomplished and those results are presented in the appended manuscript:

L. Fan, C.V. Pepicelli, C. C. Dibble, W. Catbagan, J. L. Zarycki, R. Laciak, J. Gipp, A. Shaw, M. L.G. Lamm4, A. Munoz, R. Lipinski, J. B. Thrasher and W. Bushman: Hedgehog Signaling Promotes Prostate Xenograft Tumor Growth Endocrinology. 2004 Aug;145(8):3961-70

Supporting work, describing the expression of Shh in the developing human prostate was described in the appended manuscript:

D. H. Barnett, H. Y. Huang, X. R. Wu, P. M. Bak, R. Laciak, E. Shapiro, and W. Bushman: The Human Prostate Expresses Sonic Hedgehog During Fetal Development. J Urol, 2002 Nov:168(5):2206-10.

Ours were the first human studies to comprehensively characterize hedgehog signaling in the human prostate and prostate cancer and the first published study of the role of hedgehog signaling in tumor growth. Our contribution to the field is reflected in our invitation to contribute a review of this subject to the Second Edition of Prostate Cancer: Novel Biology, Genetics and Therapy.

Bushman W. Hedgehog Signaling in Growth and Development. Prostate Cancer: Novel Biology, Genetics and Therapy (in press)

Key Research Accomplishments:

- We have shown in a survey of adult human prostate tissues that substantial levels of hedgehog signaling exist in normal hyperplastic and malignant tissue.

- In cancer specimens Shh expression is localized to the tumor epithelium while Gli1 expression is localized to the tumor stroma. This tight correlation between the levels of Shh and Gli1 expression would suggest active signaling between the tissue layers.

- We have shown that Shh expressed by LNCaP cells in the xenograft tumor model activates Gli1 expression in the tumor stroma.

- Shh over expression in LNCaP cells accelerates tumor growth. This is associated with a dramatic up-regulation of stromal Gli1 expression. Together these implicate Shh as an important paracrine activator in prostate cancer.

Reportable Outcomes:

1) Manuscripts describing these results has been submitted for publication (appended).

2) Based on this work a post-doctoral fellow, Mark Koeppel has applied for and received funding from the Department of Defense.

Conclusions:

This work has identified, for the first time, Shh signaling as an important paracrine activator in prostate cancer growth. Our studies have shown that this signaling pathway is active in human prostate cancer and that it dramatically accelerates tumor growth in a xenograft model. Subsequent to our publications, three additional papers appears also showing that hedgehog signaling promotes tumor growth and providing proof of principle for targeting hedgehog signaling in the treatment of prostate cancer. Shh signaling is a demonstrated target for chemical inhibition and has significant chemotherapeutic applications in cancer. These findings therefore have great importance for human health. They identify Shh signaling as a potential target for therapeutic intervention to slow or arrest prostate tumor growth – and provide patients with prostate tumor growth extended life expectancy and increased quality of life.

Personnel:
Wade A. Bushman, MD, PhD
Crist H. Cook, BS
Jerry J. Gipp, PhD

0013-7227/04/$15.00/0
Printed in U.S.A.

Endocrinology 145(8):3961–3970

doi: 10.1210/en.2004-0079

APPENDIX 1

Hedgehog Signaling Promotes Prostate Xenograft Tumor Growth

LIAN FAN, CARMEN V. PEPICELLI, CHRISTIAN C. DIBBLE, WINNIE CATBAGAN, JODI L. ZARYCKI, ROBERT LACIAK, JERRY GIPP, AUBIE SHAW, MARILYN L. G. LAMM, ALEJANDRO MUNOZ, ROBERT LIPINSKI, J. BRANTLEY THRASHER, AND WADE BUSHMAN

Curis, Inc. (C.V.P., C.C.D., J.L.Z.), Oncology Group, Cambridge, Massachusetts 02163; Division of Urology/Department of Surgery (J.G., A.S., A.M., R.Li., W.B.), University of Wisconsin, Madison, Wisconsin 53792; and Division of Urology (J.B.T.), University of Kansas Medical Center, Kansas City, Kansas 66113; and Northwestern University Feinberg School of Medicine (L.F., W.C., R.La., M.L.G.L.), Chicago, Illinois 60611

During fetal prostate development, Sonic hedgehog (*Shh*) expression by the urogenital sinus epithelium activates *Gli-1* expression in the adjacent mesenchyme and promotes outgrowth of the nascent ducts. *Shh* signaling is down-regulated at the conclusion of prostate ductal development. However, a survey of adult human prostate tissues reveals substantial levels of Shh signaling in normal, hyperplasic, and malignant prostate tissue. In cancer specimens, the *Shh* expression is localized to the tumor epithelium, whereas *Gli-1* expression is localized to the tumor stroma. Tight correlation between the levels of *Shh* and *Gli-1* expression suggests active signaling between the tissue layers. To determine whether *Shh-Gli-1* signaling could be functionally important for tumor growth and progression, we performed experiments with the LNCaP xenograft tumor model and demonstrated that: 1) *Shh* expressed by LNCaP tumor cells activates *Gli-1* expression in the tumor stroma, 2) genetically engineered *Shh* overexpression in LNCaP cells leads to increased tumor stromal *Gli-1* expression, and 3) *Shh* overexpression dramatically accelerates tumor growth. These data suggest that hedgehog signaling from prostate cancer cells to the stroma can elicit the expression of paracrine signals, which promote tumor growth. (*Endocrinology* 145: 3961–3970, 2004)

THE PROSTATE GLAND is composed of a secretory epithelial parenchyma and a stroma consisting of smooth muscle cells and fibroblasts (1, 2). The stromal cells elaborate components of the extracellular matrix and paracrine factors that regulate epithelial cell proliferation and differentiation (3). The role of mesenchyme in directing growth and morphogenesis during embryonic prostate development is well established (4). Similarly, a growing body of evidence indicates that the stroma may undergo phenotypic and/or genotypic changes that enhance prostate cancer growth (5, 6). It has been shown, for example, that coinjection of prostate cancer-derived fibroblasts with tumorigenic epithelial cells into nude mice enhances tumor take and growth (7–12). Tumors may be able to recruit normal stromal cells to support tumor growth by inducing expression of a variety of angiogenic and growth factors in a paracrine fashion (reviewed in Ref. 13). The stromal reaction in cancer resembles the activity of stromal cells in wound healing and may create conditions that favor tumor progression (3).

Hedgehog proteins in the prostate

Sonic hedgehog (Shh) is a secreted protein that acts as a potent inducer of morphogenesis and growth in diverse structures of the developing embryo (14–19). All known biological activity is associated with the N-terminal fragment of the protein (20, 21). Shh exerts its effects by activating gene transcription in target cells expressing the hedgehog receptor *Patched* (*Ptc-1*) (22). This interaction initiates a complex intracellular signal transduction cascade that activates the transcription factor *Gli-1* (23), one of three mammalian *Gli* genes related to the Drosophila segment polarity gene Cubitus interruptus (24). *Gli-1* activation results in increased expression of *Gli-1* itself, Ptc-1, and target genes that regulate proliferation, differentiation, and extracellular matrix interactions (25). *Gli-2* encodes a transcriptional regulator that shares extensive homology with *Gli-1* and may provide functional redundancy in the transcriptional response to Shh signaling. *Gli-3* is believed to provide both positive and negative regulatory control over the expression of *Shh* target genes (reviewed in Ref. 26).

Studies of prostate development suggest that Hedgehog signaling is critical for normal ductal morphogenesis (15, 27, 28). Epithelial *Shh* expression is concentrated at sites of ductal bud formation and the tips of the growing ducts in which it activates *Gli-1* and *Gli2* expression in the adjacent mesenchyme. Negation of *Shh* signaling impairs the activation of *Gli-1* and *Gli-2* expression and inhibits ductal outgrowth (14–15, 28). Because this effect entails primarily an inhibition of epithelial cell proliferation, it suggested that epithelial *Shh* expression activates stromal-mediated paracrine signals that feed back and stimulate epithelial cell proliferation (15).

LNCaP cells are human prostatic epithelial cells derived from a metastatic supraclavicular lymph node (29). The

Abbreviations: ANCOVA, Analysis of covariance; BPH, benign prostate hyperplasia; EGFP, enhanced green fluorescent protein; FBS, fetal bovine serum; GAPDH, glyceraldehyde-3-phosphate dehydrogenase; GFP, green fluorescent protein; *Ptc-1*, hedgehog receptor *Patched*; Shh, Sonic hedgehog.

Endocrinology is published monthly by The Endocrine Society (http://www.endo-society.org), the foremost professional society serving the endocrine community.

LNCaP cell line forms xenograft tumors at high efficiency when coinjected with Matrigel into nude mice (30). The xenograft tumors are composed of (human) LNCaP prostate cancer cells and host (mouse) derived stromal cells. We have taken advantage of this model to examine the influence of *Shh* signaling on prostate tumor growth. Our studies show that *Shh* expressed by LNCaP cells activates *Gli-1* gene expression in host-derived stromal cells and that overexpression of *Shh* in the prostate cancer cells up-regulates stromal *Gli-1* gene expression *in vivo* and accelerates xenograft prostate tumor growth. All of the evidence from these xenograft studies argues against autocrine signaling and suggests that *Shh* acts through the stroma to stimulate tumor cell proliferation.

Materials and Methods

Plasmids and cell lines

The human *Shh* overexpression vector, pIRES2-h*Shh*-enhanced green fluorescent protein (EGFP), was made by cloning a 1.55-kb human *Shh* cDNA fragment (provided by Dr. Cliff Tabin, Harvard University, Boston, MA) into the *Eco*RI site of the cytomegalovirus promoter driven pIRES2-EGFP (Clontech, Palo Alto, CA). LNCaP cells (American Type Culture Collection, Manassas, Va) were transfected with pIRES2-h*Shh*-EGFP or pIRES2-EGFP vector alone using Lipofectin (Life Technologies, Inc., Grand Island, NY) and subcloned by limiting dilution. One high *Shh* expressor clone [LNCaP$^{Shh(H)}$] and one medium *Shh* expressor clone [LNCaP$^{Shh(M)}$] were identified by green fluorescent protein (GFP) expression, and their *Shh* expression levels were confirmed by RT-PCR and Western blot.

LNCaP proliferation

Cells were plated at a density of 2×10^4 cells/well in 24-well plates in complete media [RPMI 1640 containing 2 mM L-glutamine + 1.5 g/liter sodium bicarbonate + 4.5 g/liter glucose + 10 mM HEPES + 1 mM sodium pyruvate + 10% fetal bovine serum (FBS)]. Cells were counted on a counter model ZF analyzer (Coulter, Fullerton, CA). Cell death, determined by Trypan blue exclusion, did not change under any of the treatment conditions. For cyclopamine experiments, subconfluent LNCaP and p2$^{Ptc-/-}$ (31) cells were incubated in medium containing 2% calf serum with or without 5 μM cyclopamine (Toronto Research Chemicals, Ontario) for 7 d.

Xenograft model

All animal experiments were conducted in accord with institutional policies and Institutional Animal Care and Use Committee guidelines. LNCaP xenograft tumors were created by sc coinjection of LNCaP cells (1×10^6 in 250 μl PBS) with 250 μl Matrigel into both flanks of adult male nude CD-1 mice (Charles River Laboratories, Wilmington. MA). Ten mice each were injected with each of the four cell lines. Tumors were measured weekly with a caliper and tumor volumes were calculated according to the formula (length × width × depth × 0.5236) (32). The mice were followed up for 11 wk, although some cell lines experienced high mortality beginning at wk 9.

RT-PCR

Semiquantitative RT-PCR performed as previously described (16), using message for the ribosomal subunit protein, *RPL-19*, as an internal standard. Real-time quantitative RT-PCR was performed using TaqMan instrumentation (Applied Biosystems, Foster City, CA) and used gene-specific primers and glyceraldehyde-3-phosphate dehydrogenase (GAPDH) as an internal standard. Total RNA isolated from cryopulverized tissue with Trizol (Gibco-BRL, Gaithersburg, MD) was subjected to reverse transcription using standard protocols. Species-specific primers for human *Shh* and mouse *Gli* genes and *Ptc-1* were used to localize expression to the epithelial and stromal components of xenograft tumors. Primer sequences were as follows:

Human *GAPDH* forward: CCA CAT CGC TCA GAC ACC AT, reverse: GCA ACA ATA TCC ACT TTA CCA GAG TTA A; human *Shh* forward: AAG GAC AAG TTG AAC GCT TTG G, reverse: TCG GTC ACC CGC AGT TTC; human *Gli-1* forward: AAT GCT GCC ATG GAT GCT AGA, reverse: GAG TAT CAG TAG GTG GGA AGT CCA TAT; human *Gli-2* forward: AAG AAA GTG ATG ATG CGA TGT CTA A, reverse: TGT CGG TAA AGC AGC ACA TGT AT; human *Gli-3* forward: ATC ATT CAG AAC CTT TCC CAT AGC, reverse: TAG GGA GGT CAG CAA AGA ACT CAT; human *Ptc-1* forward: CGC TGG GAC TGC TCC AAG T, reverse: GAG TTG TTG CAG CGT TAA AGG AA; mouse *GAPDH* forward: AGC CTC GTC CCG TAG ACA AAA T, reverse: CCG TGA GTG GAG TCA TAC TGG A; mouse *Shh* forward: AAT GCC TTG GCC ATC TCT GT, reverse: GCT CGA CCC TCA TAG TGT AGA GAC T; mouse *Gli-1* forward: GGA AGT CCT ATT CAC GCC TTG A, reverse: CAA CCT TCT TGC TCA CAC ATG TAA G; mouse *Gli-2* forward: TCC ATG AAG CTC GTC AAG GTT, reverse: GCA AGT AAC TGA GGA GAC TAC AAT ATC C; mouse *Gli-3* forward: AGC CCA AGT ATT ATT CAG AAC CTT TC, reverse: ATG GAT AGG GAT TGG GAA TGG; mouse *Ptc-1* forward: CTC TGG AGC AGA TTT CCA AGG, reverse: TGC CGC AGT TCT TTT GAA TG.

Each PCR was run in duplicate and according to the manufacturer's recommendations and default settings.

Western blots

Lysates for Western blot analysis were prepared as previously described (33). Total protein (10–20 μg) was run on 14% SDS-PAGE gel, transferred to nitrocellulose membrane (Amersham Corp., Piscataway, NJ), incubated with 1:200 goat antihuman Shh N-terminal antibody (catalog no. SC-1194, Santa Cruz Biotechnology, Santa Cruz, CA) followed by 1:5000 horseradish peroxidase-conjugated donkey antigoat IgG (Santa Cruz, catalog no. SC-2056) and developed by enhanced chemiluminescence (Amersham Corp.).

Histology and radioactive in situ hybridization

Tumor tissues were fixed in 4% paraformaldehyde overnight at 4 C, embedded in paraffin, sectioned at 5 μm thickness, and stained with hematoxylin and eosin. *In situ* hybridizations were performed on paraformaldehyde-fixed, paraffin-embedded histological sections as described previously (34). Mitotic indices were determined by scoring epithelial mitotic figures in 10 randomly selected high-power fields from representative sections of two xenograft tumors from each type. All counted mitotic figures were in tumor cells; no stromal mitotic figures were observed.

Gli-luc assay

C3H10T1/2 cells (ATCC) carrying a hedgehog-responsive reporter gene construct (35) were cocultured with either LNCaP or LNCaP$^{Shh(H)}$ cells (10,000 each per well) overnight in medium containing 10% FBS. The next day, the plates were changed to medium with 0.5% FBS. After 48 h, plates were assayed for luciferase activity with the LucLite kit (Packard, Meriden, CT).

Human tissues

Pooled fetal prostate RNA from 20–22 wk gestation and fetal brain RNA was obtained from Invitrogen (Carlsbad, CA). Adult human prostate tissues were obtained at Northwestern University from the following sources: 1) normal prostate tissues from organ donors at the time of organ harvest; 2) prostate cancer tissues from transurethral surgery in men with clinically advanced prostate cancer or by focal excision of tumor tissue from radical prostatectomy specimens; or 3) benign prostate hyperplasia (BPH) tissues from transurethral or simple prostatectomy. In each case, the diagnostic designation was histologically confirmed. Paired prostate cancer/ benign prostate tissue specimens were provided by the Tissue and Serum Repository (Kansas Cancer Institute, University of Kansas Medical Center, Kansas City, KS). After removal of the prostate from men undergoing radical prostatectomy for clinically localized prostate cancer, core biopsies were performed of presumed tumor and the equivalent site on the contralateral side of the specimen. Of the 20 specimens processed in this way, 11 pairs of tumor and benign

tissue from the same patient were confirmed by histologic examination. Only these 11 sets were included in the final analysis. All procedures for tissue acquisition and analysis were approved by the institutional review boards of Northwestern University and Kansas University Medical Center.

Statistical analysis

Cell line growth culture. To assess growth of the four cell lines, a Gompertz growth model was fitted to each line. Day 0 cell counts were used as a baseline; counts for each line in subsequent days were expressed as percentages with respect to the d 0 average count. Natural (base e) logarithms of the percentages were obtained to make the variability across time and cell lines more homogeneous. A Gompertz model with line-specific asymptote and growth rate was estimated via Gauss-Newton optimization, as implemented in R v1.6.2 (36). Model assumptions were assessed via residual plots, and, if warranted, parameter significance was tested via the approximate *t* test. Nonsignificant parameters were excluded and the model was refit.

Mouse tumor growth. Tumor size (cubic millimeters) was plotted against time for each mouse, with both sides combined. Mice that failed to reliably establish a tumor were not included in the analysis. Because straight lines provided a reasonably accurate summary representation of the growth patterns, least squares fits were obtained for each mouse by regressing tumor size at each time point and combining both sides. To assess differences in growth, the slopes of the regression lines were analyzed via a one-way nonparametric ANOVA (Kruskal Wallis) by ranking the slopes and performing an ANOVA on the ranks. All six pairwise comparisons between the cell least-squares mean rank were performed. Mitotic indices were compared by taking square roots of mitotic counts to stabilize the variance. Significant differences in the overall ANOVA ($P = 0.04$) were further evaluated by split-plot models.

Human tissues. Gene expression analysis provided two sets of data. Data set 1 (DS1) consisted of 19 adult male prostate specimens: normal (n = 7), prostate cancer (n = 6), and BPH (n = 6). Data set 2 (DS2) consisted of 11 paired tissues obtained at the University of Kansas Medical Center. Data from DS1 and DS2 were combined for statistical analysis: normal prostate (N, n = 7), BPH (n = 6), prostate cancer (PC, n = 6), tumor (T, n = 11), and benign (B, n = 11). Differences in the mean gene expression among groups were tested with a one-way ANOVA (completely randomized design). The residuals were examined for evidence of violations in the assumptions. If needed, variance-stabilizing transformations were used. If the overall P value for the ANOVA was significant, pairwise contrasts were obtained for all possible group pairs. No adjustment was made for testing all contrasts. To assess whether *Shh* should be incorporated as a covariate, analysis of covariance (ANCOVA) was used for each of the three *Gli* genes. The model allowed for the possibility of differences in the intercept and the slope across groups. Model fit diagnostics were obtained via graphical assessment of the residuals. If warranted, transformations were used to ensure the model assumptions were not violated.

The plots and Gompertz fits were generated in R version 1.6.25.1 (36). The ANOVA, ANCOVA, and Kruskal-Wallis analysis models were fit in SAS (release 6.12, SAS Institute, Cary, NC) (37).

Results

Expression of Shh and Gli in the adult human prostate

Shh is expressed in the human fetal prostate most abundantly between 11 and 16 wk of gestation, a period of ductal budding and intense ductal morphogenesis, and is markedly diminished by 34 wk of gestation (16). An initial semiquantitative RT-PCR survey of *Shh* and *Gli-1* expression in three normal adult prostate specimens (18, 30, and 45 yr) and eight specimens of high grade (Gleason 8–10) prostate carcinoma obtained by channel transurethral resection of the prostate, including two hormone-refractory tumors, revealed increased *Shh* and *Gli-1* expression in the majority of the cancer tissues and an apparent correlation between the intensity of *Shh* and *Gli-1* expression in the individual specimens (data not shown). These preliminary data encouraged us to more comprehensively characterize *Shh* and *Gli* gene expression in the human prostate. Two separate surveys were performed. The first compared *Shh* and *Gli* gene expression in seven normal prostate (N) specimens from organ donors 15–28 yr old, six BPH specimens obtained by TURP (n = 4) or open prostatectomy (n = 2), and six prostate cancer (PC) specimens obtained from glands removed by radical prostatectomy. The purpose of this survey design was to compare gene expression in normal prostate tissue from young adult men (N), in hyperplastic (benign) tissue from men without prostate cancer (BPH), and in specimens of human prostate cancer (PC). Expression of *Shh*, *Gli-1*, *Gli-2*, and *Gli-3* was assayed by quantitative real-time RT-PCR and normalized to an internal expression standard of robust developmental *Shh* signaling activity, fetal brain RNA. This survey revealed that *Shh* expression is generally abundant in both benign (N and BPH) and cancer (PC) specimens (Fig. 1). Expression levels varied over a wide range. For statistical analysis of expression in the different groups, logarithmic and rank transformations were used to satisfy the assumptions of normality and homogeneous variance across groups. There was little difference between the two, so only the results for the logarithmically transformed (base *e*) expressions are shown (Fig. 1A). ANOVA revealed no significant differences in levels of *Shh* expression ($P = 0.991$) or *Gli-1* expression ($P = 0.802$) in the normal (N) and BPH specimens. Mean *Shh* and *Gli-1* expression was nearly an order of magnitude higher in the cancer specimens (PC), compared with normal (N) and BPH, but given the wide variation in expression levels and the relatively small number of specimens examined, the differences were not statistically significant. For *Gli-2* there were significant differences, with N different from both PC ($P = 0.0279$) and BPH ($P = 0.0068$).

The second survey was performed on a different group of patients with prostate cancer to determine whether there is relatively higher Shh expression in a focus of cancer, compared with the background expression in zone-homologous nonmalignant prostate tissue from the same gland. Paired specimens of tumor (T) and benign (B) tissue from 11 men undergoing radical prostatectomy were obtained by matching histologically confirmed tumor with histologically confirmed benign tissue obtained from the contralateral lobe. Statistical analysis revealed no significant differences in *Shh* or *Gli* gene expression between the cancer specimens and zone homologous tissues from the same group of patients (Fig. 1A, T *vs.* B; $P = 0.4645$).

Active Shh signaling between epithelium and stroma

To determine whether the level of *Shh* and *Gli-1* identified in the human prostate specimens is physiologically significant, we compared their expression to that seen in fetal brain where *Shh* signaling is known to play a critically important role in stimulating growth. Expression of *Shh* and *Gli-1* in matched specimens from patients with prostate cancer (T and B) was typically the same order of magnitude as the fetal brain or greater (Fig. 2, A and B). *In situ* hybridization localized *Shh* expression to the epithelium and *Gli-1* expression

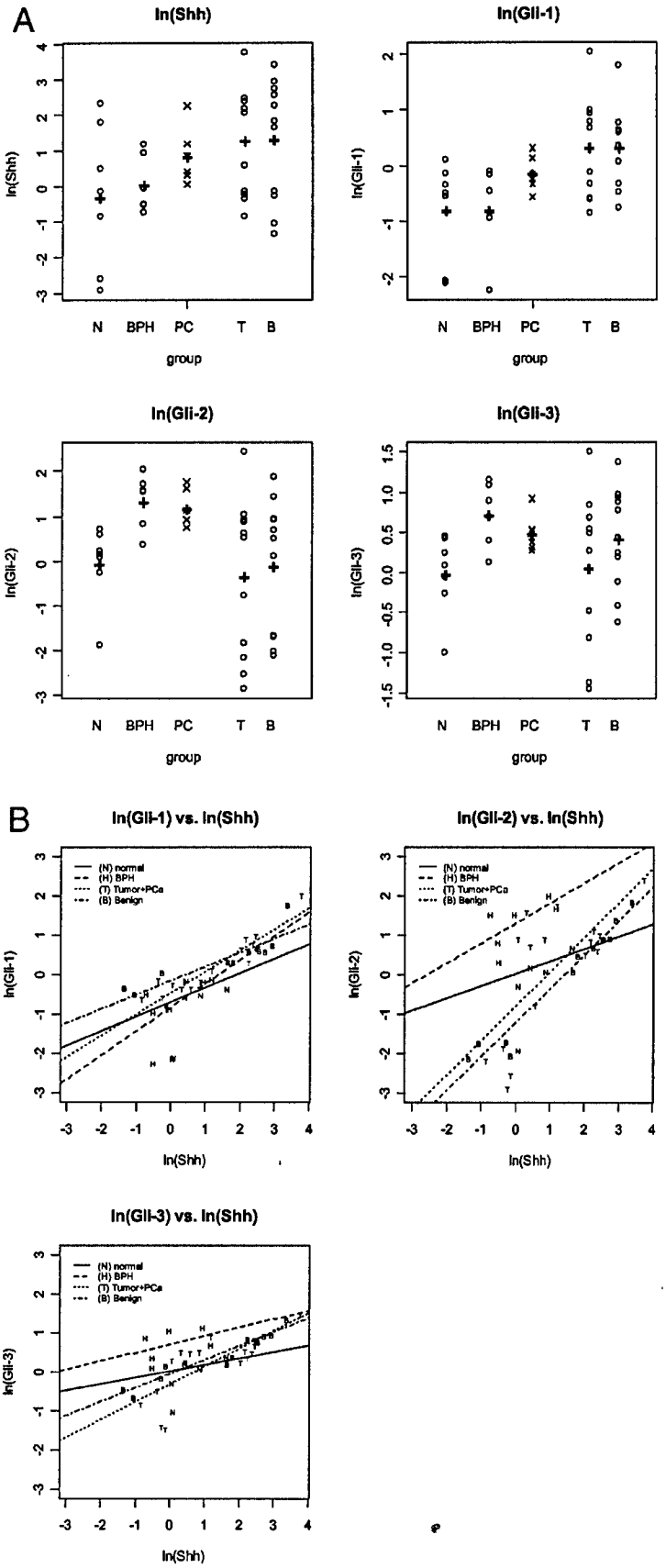

FIG. 1. A, Natural logarithms of *Shh, Gli-1, Gli-2,* and *Gli-3* gene expression data from RT-PCR analysis for each of the five groups (N, normal prostate; BPH; PC, prostate cancer; T, tumor; and B, benign). The mean value of each group is indicated (+). B, Plots of *log(Shh) vs. log(Gli-1), log(Gli-2),* and *log(Gli-3)* show a linear relationship between *Shh* and each of the *Gli* genes.

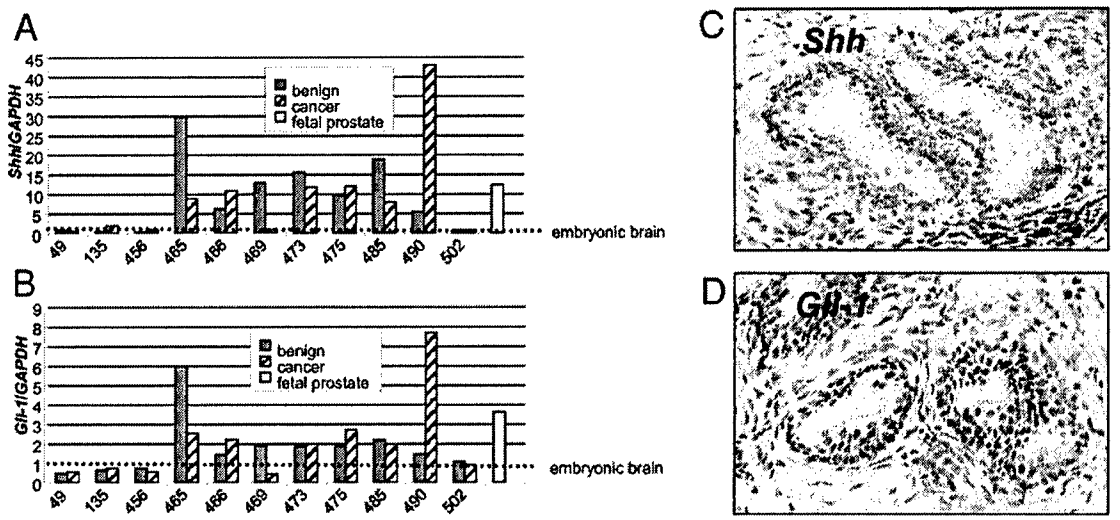

FIG. 2. A and B, Quantitative RT-PCR comparison of *Shh* expression and Gli-1 expression in matched tumor (*hatched*) and benign (*gray*) specimens from patients with prostate cancer. Each numbered pair represents histologically confirmed tumor and benign zone-homologous prostate tissue from prostates removed by radical prostatectomy. Note the generally abundant level of *Shh* and *Gli-1* expression in the prostate specimens, compared with the human fetal brain control, the very high levels of hedgehog signaling in matched sets 465–490, and the tight correlation between relative levels of *Shh* and *Gli-1* expression in individual specimens. C and D, Radioactive *in situ* hybridization analysis for *Shh* (C) and *Gli-1* (D) in tissue sections from a human prostate cancer specimen. *Shh* and *Gli-1* expression (*red* and *pink labeling*) localized to the tumor epithelium and periductal stroma, respectively. Expression of the indicated genes was investigated in paraffin sections of primary tumors. Bright-field and corresponding dark-field images were superimposed and radioactive signals highlighted with *artificial color*.

to the periglandular stroma (Fig. 2, C and D). The same pattern of localization was demonstrated in multiple specimens of prostate cancer and benign prostate tissue (data not shown). This distribution echoes the localization of the Shh and Gli-1 to the epithelium and mesenchyme in the developing prostate. Comparing the relative levels of *Shh* expression in Fig. 2A to *Gli-1* expression in the corresponding specimens in Fig. 2B reveals an apparent correlation. ANCOVA (Fig. 1B) revealed a highly significant association between *Shh* and *Gli-1* expression ($P = 0.0001$) in normal, BPH, and prostate cancer tissue groups. This association is equivalent in all subgroups and suggests that epithelial *Shh* activity determines the stromal expression of *Gli-1*. The slopes do not differ across groups ($P = 0.3015$), but the group-specific intercepts do differ ($P = 0.0357$). Therefore, log (*Gli-1*) may be described by log (*Shh*) via a set of parallel straight lines with different intercepts for each group. ANCOVA revealed a similar correlation between *Shh* expression and expression of *Gli-2* and *Gli-3* (Fig. 1B). Again, the slopes for the different groups are not significantly different for *Gli-2* and *Gli-3* ($P = 0.0853$ and $P = 0.1260$, respectively) but both log (*Gli-2*) and log (*Gli-3*) may be described by (*Shh*) as straight line predictor ($P < 0.0002$) with varying intercepts ($P < 0.001$).

LNCaP Shh expression drives stromal Gli-1 expression in xenograft tumors

LNCaP cells were stably transfected with a GFP expression vector containing the human *Shh* cDNA under the control of a cytomegalovirus promoter. Two clones exhibiting different degrees of *Shh* overexpression [$LNCaP^{Shh(M)}$ and $LNCaP^{Shh(H)}$ medium and high expression, respectively] by RT-PCR and Western blot analysis, compared with a clone transfected with vector only ($LNCaP^{GFP}$) and the parent cell line, were selected for further study. Expression and secretion of functional Shh peptide by the *Shh*-overexpressing cells was confirmed by coculture with a *Gli*-luciferase reporter cell line (37) (Fig. 3A). However, *Shh* overexpression was not associated with activation of human *Ptc-1*, *Gli-1*, or *Gli-2* in monolayer culture of LNCaP cells alone (Fig. 3, B–D), arguing against autocrine signaling activity. The *Shh*-overexpressing and control cells exhibited identical morphology (not shown), and no significant differences in growth rate ($P > 0.112$) or maximal growth ($P > 0.739$) in culture (Fig. 3E). To exclude a contribution of ligand-independent (autocrine) activation of hedgehog signaling in the parental LNCaP, we used a chemical inhibitor of hedgehog signaling, cyclopamine, which interferes with activation of the postreceptor intracellular signal transduction mechanism (31). The LNCaP cell line exhibited no inhibition of LNCaP cell proliferation by 5 μM cyclopamine, a concentration that significantly inhibits proliferation of *Ptc−/−* cells (data not shown) (31).

When coinjected with Matrigel, LNCaP parent and *Shh*-overexpressing cell lines both form xenograft tumors consisting of nests of human prostate cancer cells and an intervening, well-vascularized fibroblastic stroma derived from the host mouse (30). The tumors appeared indistinguishable (Fig. 4), and review by a urologic pathologist identified no differences between xenografts made with the LNCaP parent cell line or cells overexpressing Shh. Human- and mouse-specific primers were used to assay for *Ptc-1*, *Gli-1*, and *Gli-2* expression to determine the target of *Shh* signaling. Xenograft tumors made with LNCaP parent and Shh-overexpressing cell lines show barely detectable human *Ptc-1* expression and no human *Gli-1* expression (not shown). In contrast, mouse *Ptc-1* and *Gli-1* were expressed in xenograft tumors made with the LNCaP parent cell line and demonstrated dramatically increased expression in xenograft tumors made

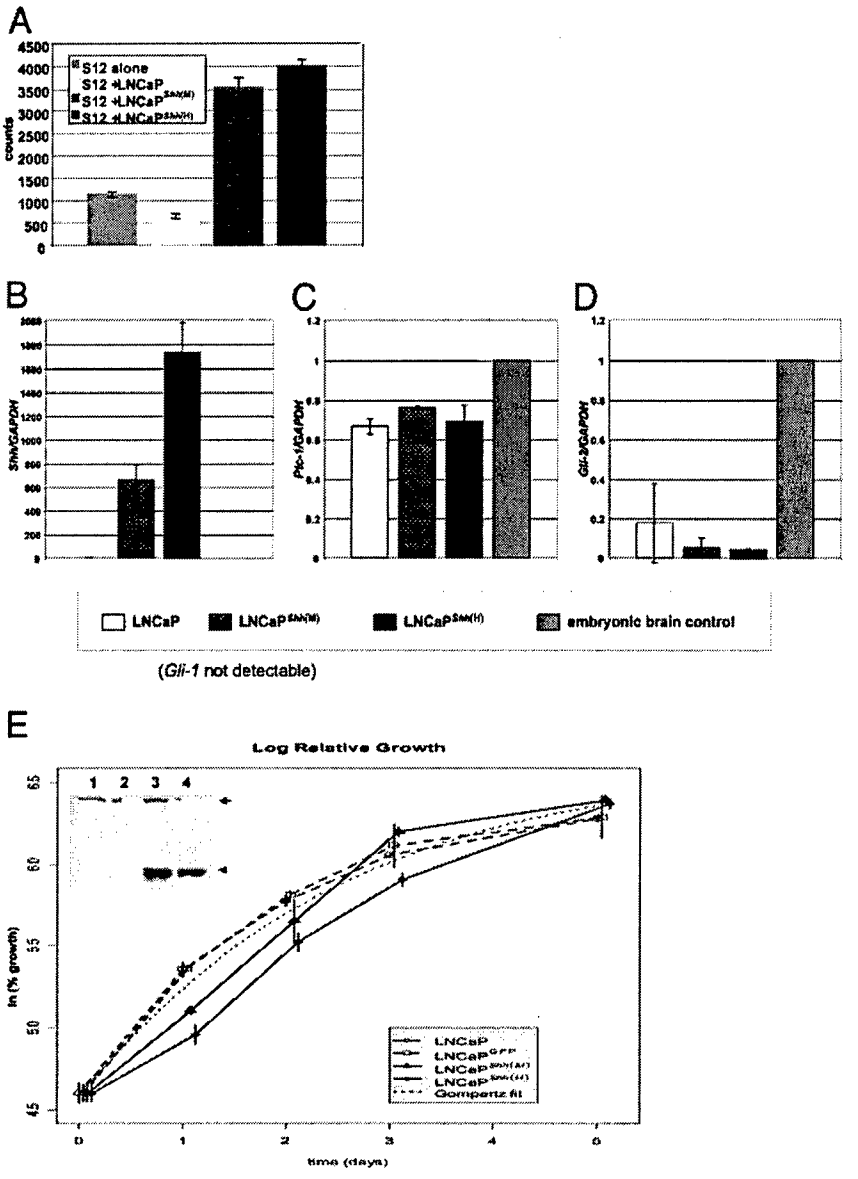

FIG. 3. A, S12 cells, C3H10T1/2 cells carrying a hedgehog-responsive reporter gene construct (35), were cultured alone or cocultured with LNCaP, LNCaP$^{Shh(M)}$, or LNCaP$^{Shh(H)}$ cells overnight. *Gli-1*-luciferase reporter assay confirms production, processing, and secretion of functional hedgehog ligand by LNCaP cells overexpressing Shh. B–D, *Shh* overexpression is not associated with autocrine stimulation of *Ptc-1*, *Gli-1*, or *Gli-2* expression in the LNCaP cells. B, Shh expression in the LNCaP parent cell line by quantitative RT-PCR is low relative to the embryonic brain control (which equals 1 and is too low to be visible in this graph). Shh expression in LNCaP$^{Shh(M)}$ and LNCaP$^{Shh(H)}$ cell lines is approximately three orders of magnitude greater than embryonic brain. *Gli-1* expression is undetectable both in the parent and overexpresser cell lines (data not shown). C and D, Expression of neither human *Ptc-1* nor *Gli-2* is increased by Shh overexpression. E, Shh overexpression is not associated with any change in growth rate in culture. Log-relative growth in culture for four LNCaP cell lines, with Gompertz fit (*dotted line*). *Inset*, Western blotting for Shh peptide in the LNCaP parent, LNCaP^{GFP}, LNCaP$^{Shh(M)}$, and LNCaP$^{Shh(H)}$ cell lines (lanes 1–4, respectively; *arrow* indicates lane origin) confirming abundant levels of the 19-kDa peptide (*arrowhead*) in the LNCaP$^{Shh(M)}$ and LNCaP$^{Shh(H)}$ cell lines. Expression in the LNCaP parent and LNCaP^{GFP} cell lines is too low to be seen in the gel shown.

with cells overexpressing Shh (Fig. 5, A–D). These findings indicate that *Shh* secreted by LNCaP cells signals to mouse stromal cells present within the xenograft tumor and activates stromal cell *Ptc-1* and *Gli-1* expression in a paracrine loop. These findings were confirmed by radioactive *in situ* hybridization (Fig. 5, E–H).

Shh overexpression accelerates tumor growth

Control cells and LNCaP cells overexpressing *Shh* formed tumors with equally high take rates (80–100%) when coinjected with Matrigel. Neither demonstrated significant tumor formation even with prolonged (12 wk) follow-up when injected without Matrigel (data not shown). We therefore compared the growth rate of xenografts made by coinjection with Matrigel (Fig. 6). Compared with both the parent cell line and GFP control, the medium and high *Shh*-overexpressing xenografts both exhibit significantly increased tumor growth rates. A slower rate of growth of the GFP control than the parent cell line is thought to reflect a nonspecific difference between the clonal GFP and parent cell lines. Additional experiments using nonclonal GFP and Shh overexpresser cell lines showed a comparable increase in tumor growth rate with Shh overexpression (our unpublished observations). Histologic examination of the tumors excluded an increase in stromal proliferation as an explanation of the increased tumor growth rate because both overexpresser and control xenografts are composed of an epithelium-rich tumor with a relatively small component of stromal tissue. Mitotic figures in the tumor stroma were scarce; in contrast, mitotic figures were very common in the tumor cell component of the xenograft (see Fig. 4). Tumor cell proliferation was significantly higher in the medium and high Shh overexpressers [2.85 ± 1.7 and 2.40 ± 1.8 (mean ± SD) mitotic figures per high power field, respectively] than the GFP and LNCaP parent controls (0.35 ± 0.75 and 0.550 ±

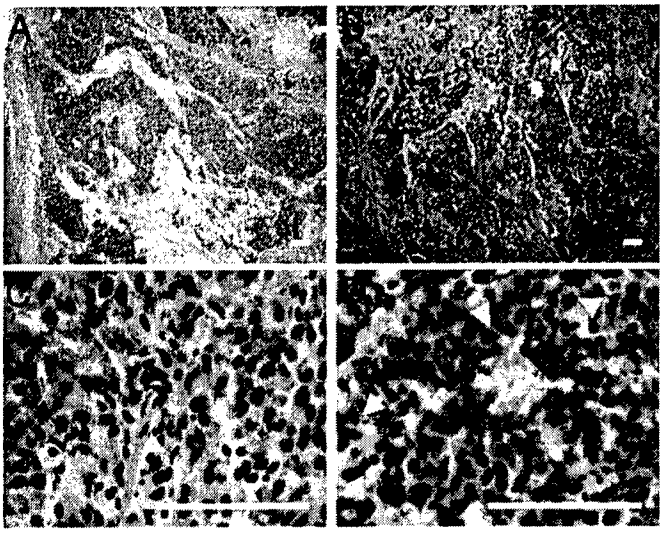

FIG. 4. Histology of xenograft tumors made with the LNCaP parent cell line (A, C) and LNCaP$^{Shh(H)}$ overexpresser (B, D). Low-power views show comparable stromal and epithelial composition in the control (A) and overexpresser (B) xenografts. High-power views show similarity in tumor cell differentiation and density. Mitotic figures (*arrow*) are evident in both the control (C) and overexpresser (D) xenografts. The size marker denotes 100 μM.

0.89, respectively; $P = 0.0016$). These data support the observation that increased tumor growth results from an increase in tumor cell proliferation. The striking contrast between the similar growth rates of the *Shh*-overexpressing and control cells in culture and the marked differences in xenograft growth rates suggests that *Shh* overexpression stimulates tumor growth via a stromal mediated paracrine mechanism.

Discussion

Hedgehog signaling in normal and diseased prostate tissue

Epithelial-mesenchymal interactions driven by Hedgehog ligand are a central theme in the morphogenesis of several developing organs (38–42). Inappropriate activation of the hedgehog signaling pathway has recently emerged as a key factor in oncogenesis and hyperproliferative disease, particularly in those organs in which Shh plays an important embryologic role (reviewed in Refs. 43, 44). Dahmane *et al.* (45) observed abundant *Gli-1* expression in nine of 11 prostate cancer tissues examined and speculated that hedgehog signaling could play an important role in prostate cancer. This prompted us to more carefully examine hedgehog activity in benign and malignant adult prostate tissue. Our comparative analysis of prostate specimens from young adult men, men with BPH, and men with prostate cancer showed a trend toward higher *Shh* and *Gli-1* expression in the cancer specimens, but this trend did not reach statistical significance. Even so, we found surprisingly high expression levels in these adult tissues: *Shh* and *Gli-1* expression in most of the specimens exceeds the level of expression found in the fetal brain (see Fig. 4). This finding is in contrast to the mouse prostate in which expression in the adult is very low. The explanation may be that a wide range of histopathologic processes universally afflict the human prostate throughout the adult life span, including inflammation, hyperplasia, dysplasia atrophy, and proliferative atrophy as well as cancer. Indeed, we observed abundant Shh activity associated with foci of inflammation (our unpublished observations).

Comparison of *Shh* expression and *Gli-1* expression in biopsies from contralateral lobes of the same gland showed a surprisingly strong correlation between expression in the tumor and benign tissue from the same patient (see Fig. 4). This was true despite wide variation in the levels of *Shh* and *Gli-1* expression among individuals and suggests that the level of *Shh* signaling activity is a generalized characteristic of an individual's prostate. We observed a very tight correlation between *Shh* and *Gli-1* expression in individual specimens of benign and malignant prostate tissue (see Figs. 1B and 4). Together with localization studies showing *Shh* and *Gli-1* expression confined to the epithelium and stroma, respectively, this indicated that functional signaling by Shh from the benign epithelial and/or tumor cells drives *Gli-1* expression in the prostatic stroma. Intriguingly, the strong correlation between *Shh* and *Gli-1* in human specimens was clearly evident, even though the stromal/epithelial ratio varies significantly among specimens. This is best explained by restriction of Shh diffusion and localized signaling activity to the immediately adjacent stromal cells.

Hedgehog signaling in cancer

Ectopic activation of Sonic hedgehog signaling is a key event in the generation of sporadic (46, 47) and hereditary basal cell carcinoma (48, 49) as well as medulloblastoma (50, 51). Mice heterozygous for Ptc-1 develop medulloblastomas (52) and, under some experimental conditions, skin lesions resembling basal cell carcinoma (53). In these cancers, activation of the Hedgehog pathway is believed to induce proliferation in epithelial tumor cells via activation of cyclins and cyclin-dependent kinases (54) in an autocrine loop. Accordingly, Hedgehog antagonists are effective inhibitors of tumor growth in models of medulloblastoma (55) and basal cell carcinoma (35). Recently ligand-dependent Hedgehog signaling has been described in a subset of human small-cell lung carcinomas and small-cell lung carcinoma cell lines tested (56). Tumor growth is significantly inhibited by treatment with the natural Hedgehog antagonist cyclopamine in a xenograft model derived from one of these cell lines that is expressing Shh and Gli-1 concomitantly. Similar studies have shown Shh signaling promotes growth of pancreatic and upper gastrointestinal tumors (57, 58). These studies show evidence of autocrine signaling but also noted activation of Shh target genes (Ptc) in the reactive stroma adjacent to the tumor.

As yet there is no evidence that oncogenic mutations of the Hedgehog pathway genes *Ptc-1* or *Smo* exists in prostate cancer, and our localization studies did not show strong evidence for autocrine signaling in localized prostate cancer. Instead, our studies suggested that paracrine signaling from tumor cells to the adjacent stroma represents the major pathway of hedgehog target gene activation in prostate cancer. To examine the influence of such signaling on tumor growth, we

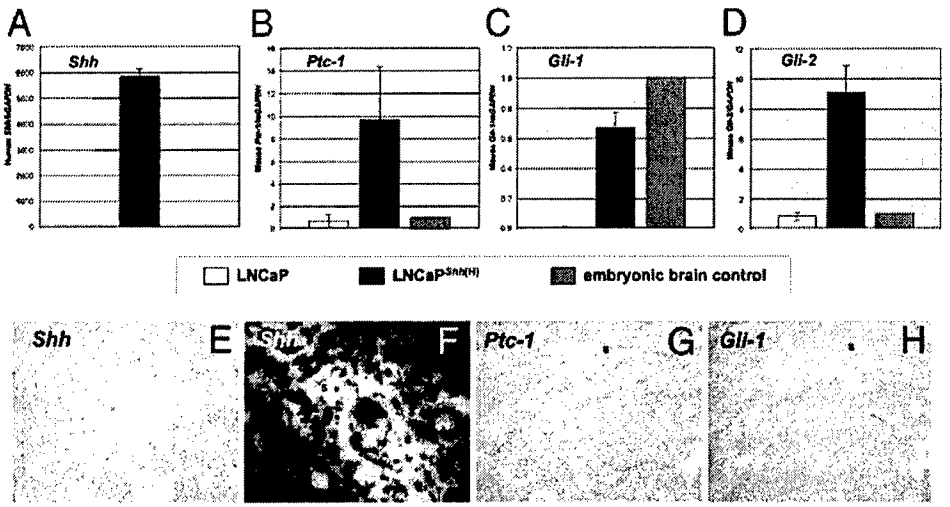

FIG. 5. A–D, Quantitative RT-PCR analysis of hedgehog pathway genes in xenograft tumors. A, *Shh* is overexpressed in LNCaP$^{Shh(H)}$ xenograft tumors. The level of expression in the parent LNCaP cell line is three orders of magnitude less and too low to be seen in this graph. B–D, Mouse *Ptc-1, Gli-1,* and *Gli-2* expression is significantly increased in overexpresser xenograft tumors. Approximately equivalent high-level mouse Ptc-1, Gli-1 and Gli-2 expression was observed in xenograft tumors made with the LNCaP$^{Shh(M)}$ and LNCaP$^{Shh(H)}$ cell lines (not shown), indicating that in the presence of high levels of Shh expression, stromal gene activation reaches a plateau that is independent of the absolute concentration of Shh protein produced by the epithelium. E–H, Localization of mouse *Ptc-1* and *Gli-1* expression. No detectable *Shh* signal is seen in the LNCaP parent cell line xenograft tumor (E). In the LNCaP$^{Shh(H)}$ xenograft, strong tumor cell *Shh* expression (F) is mirrored by mouse *Ptc-1* and *Gli-1* expression (G, H) in the tumor stroma (S). Comparable studies of the canonical LNCaP xenografts did not show significant Gli-1 or Ptc expression in the stroma (not shown). Bright-field images were captured for abundantly expressed *Shh*; the radioactive signal is visible as *black silver grains*. For Ptc-1 and Gli-1, bright-field and corresponding dark-field images were superimposed and radioactive signals filled in with *artificial color* (*red* and *pink*).

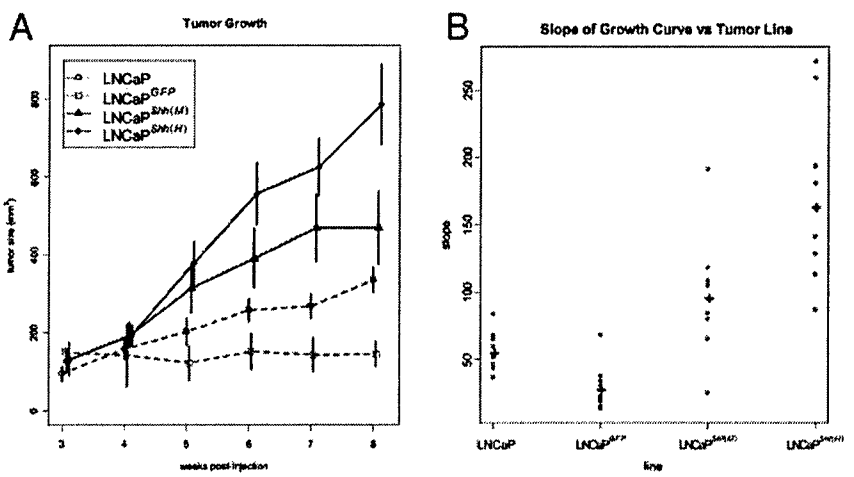

FIG. 6. Shh overexpression increases xenograft tumor growth. The LNCaP, LNCaP^{GFP}, LNCaP$^{Shh(M)}$, and LNCaP$^{Shh(H)}$ xenograft tumors were grown for 8 wk and tumor size serially determined after the appearance of visible tumors. The incidence of tumors generated with the various cell lines was comparable; in the few cases in which a tumor did not form, it was not counted in the analysis. A, Average tumor size by line. The rates of tumor growth were determined by averaging the tumor size for mice in each cell line at each time point. *Vertical bars* are ± SEM. *Points* and *lines* are offset horizontally to prevent overlap. B, Average slope for each of the individual tumor growth curves over the 3- to 8-wk period. The mean slopes (+) for each tumor group are significantly different: LNCaP *vs.* LNCaP^{GFP} ($P = 0.0047$), LNCaP$^{Shh(M)}$ ($P = 0.0084$), and LNCaP$^{Shh(H)}$ ($P = 0.0001$); LNCaP^{GFP} *vs.* LNCaP$^{Shh(M)}$ ($P = 0.0001$) and LNCaP$^{Shh(H)}$ ($P = 0.0001$); and LNCaP$^{Shh(M)}$ *vs.* LNCaP$^{Shh(H)}$ ($P = 0.002$).

used the LNCaP cell line. This cell line has relatively low endogenous Shh expression and no evidence of autocrine activation by exogenous Shh peptide. Using the LNCaP xenograft made it possible to specifically measure the effect of engineered Shh overexpression and paracrine signaling on growth of the tumor. Overexpression of *Shh* in the LNCaP xenograft significantly accelerated tumor growth by increasing the rate of tumor cell proliferation *in vivo*. Gene expression analysis of the xenografts showed a lack of Shh-induced up-regulation of human *Ptc-1, Gli-1,* and *Gli-2* expression, confirming the absence of autocrine Shh signaling activity, but showed marked up-regulation of mouse *Ptc-1, Gli-1,* and *Gli-2* expression. It follows that the effect of *Shh* overexpression on tumor cell proliferation is mediated by Gli-based activation of stromal genes and paracrine mechanisms.

One limitation of the LNCaP xenograft is the nonprostatic

origin of the tumor stromal cells. The target gene response to Shh signaling could vary with the origin and/or phenotype of the stromal cells (see below). However, we have recently shown that in xenograft tumors made by coinjecting LNCaP cells with immortalized mouse prostate stromal cells, Shh overexpression induces up-regulation of mouse *Ptc-1*, *Gli-1*, and *Gli-2* expression and accelerates tumor growth similar to what is observed in the canonical xenograft model (our unpublished observations). Yoon *et al.* (25) identified approximately 30 targets of Gli-1 transcriptional regulation, including cyclin D2, osteopontin, IGF binding protein-6, MAPK 6c, and plakoglobin, several of which are expressed in the mouse fetal prostatic mesenchyme (our unpublished observations). These and/or other paracrine regulated genes are obviously candidates for Shh-mediated activation in adult prostate stromal cells. Whereas our studies of localized prostate cancer specimens and the LNCaP xenograft highlight the role of paracrine signaling, we cannot exclude a role for autocrine activation, and studies with other prostate cancer cell lines and models will provide essential complementary perspectives. Indeed, Berman and colleagues recently demonstrated autocrine/paracrine hedgehog signaling in the PC3 and 22RV1 human prostate cancer cell lines and showed that cyclopamine inhibits growth of corresponding xenograft tumors in nude mice (Berman, D., personal communication; cited with permission).

Our survey of Hedgehog pathway genes in human prostate tissue reveals significant maintenance levels of *Shh* and *Gli* gene expression in the normal adult human prostate and comparably high levels of Hedgehog signaling in prostate cancer and benign prostatic hyperplasia. Given the lack of specificity of Shh expression for prostate cancer, how can it play an important role in cancer growth and progression? The answer may lie in the nature of the stromal response to that signal in prostate cancer. During prenatal mouse prostate development, Shh activates *Gli* gene expression in the adjacent mesenchyme, promotes epithelial proliferation and ductal growth (14, 15, 28, 29). Later in prostate development, Shh appears to inhibit growth and induce differentiation of epithelial cells into postmitotic, terminally differentiated luminal cells (17). The dichotomous actions of Shh at different stages of prostate development may be due to differing concentrations of active Shh peptide or coregulators such as activin A and TGFβ1 or a change in the state of stromal cell differentiation (17).

Rowley and colleagues (59) have shown that prostate cancer-associated stromal cells are phenotypically different from the stromal cells of the normal prostate. Cancer-associated stromal cells exhibit a myofibroblast phenotype resembling the activated stromal cell associated with wound healing. Studies of tumor-associated stromal cells have shown enhanced capacity to promote tumor growth *in vivo* (reviewed in Refs. 60, 61) and demonstrated altered expression of genes such as matrix metalloproteinases and tissue inhibitors of metalloproteinases (3). More recently tumor-associated stromal cells and normal prostate stromal cells have been shown to exhibit different responses to paracrine stimulation with pigment epithelium-derived factor (62) (Kozlowski J., personal communication). The mechanism for stromal activation has not been defined and the mechanisms by which stromal cells influence tumor growth are also not well understood. However, the distinctive character of the stromal compartment associated with prostate cancer may set the stage for a categorically different response to Shh signaling. Whereas Shh signaling in the stromal context of the normal prostate may help regulate the balance between proliferation and terminal differentiation, a similar level of signaling in the context of a cancer-associated reactive stroma may induce paracrine signals that promote tumor cell proliferation. A better understanding of the stromal response to Shh signaling in normal and malignant prostate tissue will be critical to elucidating the mechanism by which Shh signaling promotes tumor growth.

Acknowledgments

We thank Dr. James Kozlowski for samples of human prostate tissue obtained at Northwestern University, Dr. Amanda Macejko for assistance in obtaining additional samples at Northwestern University, and Jodi Ballanger of the Kansas University Medical Center tissue bank for assistance in obtaining matched pairs of benign and malignant prostate tissue. We thank Drs. Lee Rubin, Stephen Gould, and Zhou Wang for discussions and comments on the manuscript and John Lydon for expert help with histology. We also thank Dr. Terrance Oberley for providing pathologic review of the xenograft tumor specimens and David Berman for communicating results prior to publication.

Received January 23, 2004. Accepted April 26, 2004.

Address all correspondence and requests for reprints to: Wade Bushman, Division of Urology/Department of Surgery, University of Wisconsin, G5/350 Clinical Sciences Center, 600 Highland Avenue, Madison, Wisconsin. E-mail: bushman@surgery.wisc.edu.

This work was supported by grants from the Department of Defense (17-00-1-0040), the National Cancer Institute (CA 95386), National Institutes of Health (DK 056238), and CapCure.

L.F. and C.V.P. contributed equally to this work.

Current address for L.F.: Global Toxicology, Pharmacia Corporation, 4901 Searle Parkway, Q2628, Skokie, Illinois 60076.

Current address for W.C. and M.L.G.L.: Children's Memorial Institute for Education and Research, Northwestern University Feinberg School of Medicine, Chicago, Illinois 60611.

Current address for R.La.: University of Illinois College of Medicine, College of Medicine West, 1853 West Polk Street, Chicago, Illinois 60614.

References

1. **McNeal JE** 1988 Normal histology of the prostate. Am J Surg Pathol 12:619–633
2. **Castellucci E, Prayer-Galetti T, Roelofs M, Pampinella F, Faggian L, Gardiman M, Pagano F, Sartore S** 1996 Cytoskeletal and cytocontractile protein composition of stromal tissue in normal, hyperplastic, and neoplastic human prostate. An immunocytochemical study with monoclonal antibodies. Ann NY Acad Sci 784:496–508
3. **Rowley D** 1998–1999 What might a stromal response mean to prostate cancer progression? Cancer Metastasis Rev 17:411–419
4. **Cunha GR, Donjacour AA, Cooke PS, Mee S, Bigsby RM, Higgins SJ, Sugimura Y** 1987 The endocrinology and developmental biology of the prostate. Endocr Rev 8:338–362
5. **Tuxhorn JA, Ayala GE, Rowley DR** 2001 Reactive stroma in prostate cancer progression. J Urol 166:2472–2483
6. **Schor SL, Schor AM** 2001 Phenotypic and genetic alterations in mammary stroma: implications for tumor progression. Breast Cancer Res 3:373–379
7. **Camps JL, Chang SM, Hsu TC, Freeman M, Hong SJ, Zhau HE, von Eschenbach AC, Chung LW** 1990 Fibroblast-mediated acceleration of human epithelial tumor growth *in vivo*. Proc Natl Acad Sci USA 87:75–79
8. **Chung LW** 1991 Fibroblasts are critical determinants in prostatic cancer growth and dissemination. Cancer Metastasis Rev 10:263–274
9. **Gleave M, Hsieh JT, Gao CA, von Eschenbach AC, Chung LW** 1991 Acceleration of human prostate cancer growth *in vivo* by factors produced by prostate and bone fibroblasts. Cancer Res 51:3753–3761
10. **Olumi AF, Dazin P, Tlsty TD** 1998 A novel coculture technique demonstrates that normal human prostatic fibroblasts contribute to tumor formation of LNCaP cells by retarding cell death. Cancer Res 58:4525–4530

11. **Condon MS, Bosland MC** 1999 The role of stromal cells in prostate cancer development and progression. In Vivo 13:61–65
12. **Olumi AF, Grossfeld GD, Hayward SW, Carroll PR, Tlsty TD, Cunha GR** 1999 Carcinoma-associated fibroblasts direct tumor progression of initiated human prostatic epithelium. Cancer Res 59:5002–5011
13. **Hanahan D, Weinberg RA** 2000 The hallmarks of cancer. Cell 100:57–70
14. **Podlasek CA, Barnett DH, Clemens JQ, Bak PM, Bushman W** 1999 Prostate development requires Sonic hedgehog expressed by the urogenital sinus epithelium. Dev Biol 209:28–39
15. **Lamm MLG, Catbagan WS, Laciak RJ, Barnett DH, Hebner CM, Gaffield W, Walterhouse D, Iannaccone P, Bushman W** 2002 Sonic hedgehog activates mesenchymal *GLI1* expression during prostate ductal bud formation. Dev Biol 249:349–366
16. **Barnett DH, Huang HY, Wu XR, Laciak R, Shapiro E, Bushman W** 2002 The human prostate expresses sonic hedgehog during fetal development. J Urol 168:2206–2210
17. **Wang B, Shou J, Ross S, Koeppen H, de Sauvage FJ, Gao WO** 2003 Inhibition of epithelial ductal branching in the prostate by Sonic hedgehog is indirectly mediated by stromal cells. J Biol Chem 278:18506–18513
18. **Hammerschmidt M, Brook A, McMahon AP** 1997 The world according to hedgehog. Trends Genet 13:14–21
19. **McMahon AP, Ingham PW, Tabin CJ** 2003 Developmental roles and clinical significance of hedgehog signaling. Curr Top Dev Biol 53:1–114
20. **Bumcrot DA, Takada R, McMahon AP** 1995 Proteolytic processing yields two secreted forms of sonic hedgehog. Mol Cell Biol 15:2294–2303
21. **Marti E, Bumcrot DA, Takada R, McMahon AP** 1995 Requirement of 19K form of Sonic hedgehog for induction of distinct ventral cell types in CNS explants. Nature 375:322–325
22. **Goodrich LV, Johnson RL, Milenkovic L, McMahon JA, Scott MP** 1996 Conservation of the hedgehog/patched signaling pathway from flies to mice: induction of a mouse patched gene by hedgehog. Genes Dev 10:301–312
23. **Kinzler KW, Bigner SH, Bigner DD, Trent JM, Law ML, O'Brien SJ, Wong AJ, Vogelstein B** 1987 Identification of an amplified, highly expressed gene in a human glioma. Science 236:70–73
24. **Hui CC, Slusarski D, Platt KA, Holmgren R, Joyner AL** 1994 Expression of three mouse homologs of the Drosophila segment polarity gene cubitus interruptus, Gli, Gli-2, and Gli-3, in ectoderm- and mesoderm-derived tissues suggests multiple roles during postimplantation development. Dev Biol 162: 402–413
25. **Yoon JW, Kita Y, Frank DJ, Majewski RR, Konicek BA, Nobrega MA, Jacob H, Walterhouse D, Iannaccone P** 2002 Gene expression profiling leads to identification of GLI1-binding elements in target genes and a role for multiple downstream pathways in GLI1-induced cell transformation. J Biol Chem 15: 5548–5555
26. **Ingham PW, McMahon AP** 2001 Hedgehog signaling in animal development: paradigms and principles. Genes Dev 15:3059–3087
27. **Freestone SH, Marker P, Grace OC, Tomlinson DC, Cunha GR, Harnden P, Thomson AA** 2003 Sonic hedgehog regulates prostatic growth and epithelial differentiation. Dev Biol 264:352–362
28. **Berman DM, Desai N, Wang X, Karhadkar SS, Reynon M, Abate-Shen C, Beachy PA, Shen MM** 2004 Roles for Hedgehog signaling in androgen production and prostate ductal morphogenesis. Dev Biol 15:387–398
29. **Horoszewicz JS, Leong SS, Kawinski E, Karr JP, Rosenthal H, Chu TM, Mirand EA, Murphy GP** 1983 LNCaP model of human prostate carcinoma. Cancer Res 43:1809–1818
30. **Lim DJ, Liu XL, Sutkowski DM, Braun EJ, Lee C, Koslowski M** 1993 Growth of an androgen-sensitive human prostate cancer cell line, LNCaP, in nude mice. Prostate 22:109–118
31. **Taipale J, Chen J, Cooper M, Wang B, Mann R, Milenkovic L, Scott M, Beachy P** 2000 Effects of oncogenic mutations in Smoothened and Patched can be reversed by cyclopamine. Nature 406:1005–1009
32. **Janek P, Briand P, Hartman HR** 1975 The effect of estrone-progesterone treatment on cell proliferation kinetics of hormone-dependent GR mouse mammary tumors. Cancer Res 35:3698–3704
33. **Lamm MLG, Long D, Goodwin SM, Lee C** 1997 Transforming growth factor-β1 inhibits membrane-association of protein kinase C in a human prostate cancer cell line, PC3. Endocrinology 138:4657–4664
34. **Wilkinson DG, Bailes JA, McMahon AP** 1987 Expression of the proto-oncogene int-1 is restricted to specific neural cells in the developing mouse embryo. Cell 50:79–88
35. **Williams JA, Guicherit OM, Zaharian BI, Xu Y, Chai L, Wichterle H, Kon C, Gatchalian C, Porter JA, Rubin LL, Wang FY** 2003 Inhibiting the Hedgehog signaling pathway induces regression of basal cell carcinoma-like lesions. Proc Natl Acad Sci USA 100:4616–4621
36. **Ihaka R, Gentleman R** 1996 R: a language for data analysis and graphics. J Comput Graph Stat 5:299–314 (software available at: http://www.r-project.org/)
37. **SAS Institute** 1996 SAS release 6.12. Cary, NC: SAS Institute
38. **St. Jacques B, Dassule HR, Karavanova I, Botchkarev VA, Li J, Danielian PS, McMahon JA, Lewis PM, Paus R, McMahon AP** 1998 Sonic hedgehog signaling is essential for hair development. Curr Biol 8:1058–1068
39. **Litingtung Y, Lei L, Westphal H, Chiang C** 1998 Sonic hedgehog is essential to foregut development. Nat Genet 20:58–61
40. **Pepicelli CV, Lewis PM, McMahon AP** 1998 Sonic hedgehog regulates branching morphogenesis in the mammalian lung. Curr Biol 8:1083–1086
41. **Ramalho-Santos M, Melton DA, McMahon AP** 2000 Hedgehog signals regulate multiple aspects of gastrointestinal development. Development 127:2763–2772
42. **Dassule HR, Lewis P, Bei M, Maas R, McMahon AP** 2000 Sonic hedgehog regulates growth and morphogenesis of the tooth. Development 127:4775–4785
43. **Taipale J, Beachy PA** 2001 The Hedgehog and Wnt signaling pathways in cancer. Nature 411:349–354
44. **Wetmore C** 2003 Sonic hedgehog in normal and neoplastic proliferation: insight gained from human tumors and animal models. Curr Opin Genet Dev 13:34–42
45. **Dahmane N, Sanchez P, Gitton Y, Palma V, Sun T, Beyna M, Weiner H, Ruiz I, Altaba A** 2001 The Sonic hedgehog-Gli pathway regulates dorsal brain growth and tumorigenesis. Development 128:5201–5212
46. **Gailani MR, Stahle-Backdahl M, Leffell DJ, Glynn M, Zaphiropoulos PG, Pressman C, Unden AB, Dean M, Brash DE, Bale AE, Toftgard R** 1996 The role of the human homologue of Drosophila patched in sporadic basal cell carcinomas. Nat Genet 14:78–81
47. **Xie J, Murone M, Luoh SM, Ryan A, Gu Q, Zhang C, Bonifas JM, Lam CW, Hynes M, Goddard A, Rosenthal A, Epstein Jr EH, de Sauvage FJ** 1998 Activating Smoothened mutations in sporadic basal-cell carcinoma. Nature 391:90–92
48. **Hahn H, Wicking C, Zaphiropoulous PG, Gailani MR, Shanley S, Chidambaram A, Vorechovsky I, Holmberg E, Unden AB, Gillies S, Negus K, Smyth I, Pressman C, Leffell DJ, Gerrard B, Goldstein AM, Dean M, Toftgard R, Chenevix-Trench G, Wainwright B, Bale AE** 1996 Mutations of human homologue of Drosophila patched in the nevoid basal cell carcinoma syndrome. Cell 85:841–851
49. **Johnson RL, Rothman AL, Xie J, Goodrich LV, Bare JW, Bonifas JM, Quinn AG, Myers RM, Cox DR, Epstein Jr EH, Scott MP** 1996 Human homolog of patched, a candidate gene for the basal cell nevus syndrome. Science 272: 1668–1671
50. **Gorlin RJ** 1987 Nevoid basal-cell carcinoma syndrome. Medicine 66:98–113
51. **Raffel C, Jenkins RB, Frederick L, Hebrink D, Alderete B, Fults DW, James CD** 1997 Sporadic medulloblastomas contain PTCH mutations. Cancer Res 57:842–845
52. **Goodrich LV, Milenkovic L, Higgins KM, Scott MP** 1997 Altered neural cell fates and medulloblastoma in mouse patched mutants. Science 277:1109–1113
53. **Aszterbaum M, Epstein J, Oro A, Douglas V, LeBoit PE, Scott MP, Epstein Jr EH** 1999 Ultraviolet and ionizing radiation enhance the growth of BCCs and trichoblastomas in patched heterozygous knockout mice. Nat Med 5:1285–1291
54. **Duman-Scheel M, Weng L, Xin S, Du W** 2002 Hedgehog regulates cell growth and proliferation by inducing cyclin D and cyclin E. Nature 417:299–304
55. **Berman DM, Karhadkar SS, Hallahan AR, Pritchard JI, Eberhart CG, Watkins DN, Chen JK, Cooper MK, Taipale J, Olson JM, Beachy PA** 2002 Medulloblastoma growth inhibition by hedgehog pathway blockade. Science 297:1559–1561
56. **Watkins DN, Berman DM, Burkholder SG, Wang B, Beachy PA, Baylin SB** 2003 Hedgehog signaling within airway epithelial progenitors and in small-cell lung cancer. Nature 422:313–317
57. **Berman DM, Karhadkar SS, Maitra A, Montes De Oca R, Gerstenblith MR, Briggs K, Parker AR, Shimada Y, Eshleman JR, Watkins DN, Beachy PA** 2003 Widespread requirement for hedgehog ligand stimulation in growth of digestive tract tumours. Nature 425:846–851
58. **Thayer SP, di Magliano MP, Heiser PW, Nielsen CM, Roberts DJ, Lauwers GY, Qi YP, Gysin S, Fernandez-del Castillo C, Yajnik V, Antoniu B, McMahon M, Warshaw AL, Hebrok M** 2003 Hedgehog is an early and late mediator of pancreatic cancer tumorigenesis. Nature 425:851–856
59. **Tuxhorn JA, Ayala GE, Smith MJ, Smith VC, Dang TD, Rowley DR** 2002 Reactive stroma in human prostate cancer: induction of myofibroblast phenotype and extracellular matrix remodeling. Clin Cancer Res 8:2912–2923
60. **Cunha GR, Hayward SW, Wang YZ** 2002 Role of stroma in carcinogenesis of the prostate. Differentiation 70:473–485
61. **Sung SY, Chung LW** 2002 Prostate tumor-stroma interaction: molecular mechanisms and opportunities for therapeutic targeting. Differentiation 70:506–521
62. **Grayhack JT, Smith ND, Ilio K, Wambi C, Kasjanski R, Crawford SE, Doll JA, Wang Z, Lee C, Kozlowski JE** 2004 Pigment epithelium-derived factor, a human testis epididymis secretory product, promotes human prostate stromal cell growth in culture. J Urol 171:434–438

Endocrinology **is published monthly by The Endocrine Society (http://www.endo-society.org), the foremost professional society serving the endocrine community.**

0022-5347/02/1685-2206/0
THE JOURNAL OF UROLOGY®

Vol. 168, 2206–2210, November 2002
Printed in U.S.A.
DOI: 10.1097/01.ju.0000032467.50007.fc

APPENDIX 2

THE HUMAN PROSTATE EXPRESSES *SONIC HEDGEHOG* DURING FETAL DEVELOPMENT

DANIEL H. BARNETT, HONG-YING HUANG, XUE-RU WU, ROBERT LACIAK, ELLEN SHAPIRO AND WADE BUSHMAN*

From the Division of Urology, Department of Surgery, University of Wisconsin Medical School, Madison, Wisconsin, and Department of Urology, New York University School of Medicine, New York, New York

ABSTRACT

Purpose: The keynote event of prostate ductal development is the formation of epithelial buds that invade the urogenital sinus mesenchyma. Studies in mice have shown that budding requires the signaling peptide *Sonic hedgehog*, which is expressed in the epithelium of the prostatic anlagen. We report our characterization of *sonic hedgehog* (*SHH*) expression in the human fetal prostate.

Materials and Methods: Reverse transcriptase-polymerase chain reaction was performed in fetal prostate RNA isolated at 15.5 and 18 weeks of gestation, respectively. Immunostaining was performed on sections from 7 male fetuses at 9.5 to 34 and in 4 female fetuses at 9 to 18 weeks of gestation.

Results: Weak staining for *SHH* was seen in the prostatic urethra at 9.5 weeks. Intense staining was seen at 11.5 and 13 weeks in the prostatic urothelium and nascent prostatic buds. Staining was slightly diminished at 16.5, further diminished at 18 to 20 and absent at 34 weeks. *SHH* expression at 15.5 and 18 weeks was confirmed by reverse transcriptase-polymerase chain reaction assay of freshly isolated prostate tissue. Comparative *SHH* immunostaining in the female showed urothelial staining at 9 and 12 weeks with staining greatest above the entrance of the müllerian ducts. Staining diminished earlier in the female (14 weeks) than in the male and was almost absent at 18 weeks.

Conclusions: *SHH* expression in the human fetal prostate is contemporaneous with the fetal testosterone surge and with ductal budding of the prostatic urothelium. *SHH* expression is also present in the female urogenital sinus but in the absence of testosterone it is not associated with ductal budding.

KEY WORDS: prostate, gene expression, fetal development, testosterone, epithelium

Development of the human prostate. The prostate develops from the urogenital sinus in response to testosterone stimulation. The embryonic prostatic anlage initially consists of a multilayered epithelium surrounded by mesenchyma. Testosterone secretion from the fetal testis begins at 8 weeks of gestation. In a process of ductal budding that starts at 10 weeks of gestation and continues at least through 14 weeks multiple epithelial outgrowths invade the surrounding mesenchyma.[1,2] These epithelial buds form ducts that elongate and branch to form a complex ductal system. During ductal development the columnar, basal cell and neuroendocrine cell compartments of the prostate epithelium appear and the mesenchyma generates a complex stroma containing fibroblasts, smooth muscle, neural and vascular elements, and a complex extracellular matrix. Postnatal development includes a period of growth during year 1 of life, quiescence during childhood and further growth with the testosterone surge at puberty. The product of this developmental process is a secretory ductal network in a dense supporting stroma that drains into the urethra via multiple main ducts.

Prostatic ductal budding as a point of study. The molecular mechanisms regulating fetal prostate development are interesting because of their possible role in the genesis of prostatic neoplasia. Laboratory studies have identified multiple factors that may have important roles in rodent prostate development and growth. However, extrapolation of these observations to the development of the human prostate must contend with species specific differences in lobar and ductal architecture, patterns of prenatal and postnatal growth, and the stromal and epithelial composition of the adult prostate gland. We focused on a specific event in prostate morphogenesis that is similar in rodents and humans, namely ductal budding. Timms et al noted that despite the different lobar and ductal architecture of the rodent and human prostate there are striking similarities in the process of ductal budding during development.[3] Also, Cunha et al performed tissue recombination experiments that mixed human and rodent urogenital sinus mesenchyma and epithelium to show that inductive signals responsible for the induction of prostate morphogenesis are conserved across species.[4] Therefore, ductal budding serves as a point of congruence in prostate development, making it an ideal model for identifying growth regulators that exert similar actions in human and mouse fetal prostate development.

Role of sonic hedgehog in prostate development. Sonic hedgehog is the mammalian homologue of the drosophila gene hedgehog. By convention the human and mouse genes/RNA message are abbreviated as *SHH* and *Shh*, respectively, while the peptides are designated by *SHH* and *Shh*. Sonic hedgehog encodes a secreted peptide that acts as a potent inducer of growth in development of the limbs, central nervous system, lungs, craniofacial skeleton, hair, teeth, gastrointestinal tract, pituitary and genital tubercle.[5,6] Sonic hedgehog peptide acts through a membrane bound receptor (patched) on the target cell and it may activate transcription of the genes involved in cell cycle regulation and growth, such

Accepted for publication May 17, 2002.
Supported by National Institutes of Health Grants DK02426 and DK52687-01.
* Financial interest and/or other relationship with Alza and Pharmacia.

as cyclin D2, mitogen activated protein kinase 6c and plakoglobin.[5,7]

We have previously observed that *Shh* is expressed in the epithelium of the mouse urogenital sinus. Expression is most abundant in the perinatal period, when budding occurs most intensely, and declines gradually after birth to a low but detectable level in the adult prostate. Antibody blockade of *Shh* action completely inhibited glandular morphogenesis and growth.[8] Recently we reported that the chemical inhibitor of hedgehog signaling cyclopamine arrests ductal budding in the urogenital sinus cultured in vitro.[9] These studies identify *Shh* as a necessary signal for the initiation of prostate ductal budding in the mouse. We correlated our observations on mouse prostate development with human prostate development by characterizing *SHH* expression in the human fetal prostate.

MATERIALS AND METHODS

Tissues. The lower genitourinary tracts were removed from 7 human male fetuses at 9.5 to 34 weeks and from 4 female fetuses at 9 to 18 weeks of gestation. Permission to use these specimens was granted by the New York University institutional board review association. Specimens were formalin fixed and paraffin embedded. Male specimens were serially sectioned transversally at 4 μM., while female specimens were sectioned sagittally. Fresh fetal prostate tissue was obtained at 15.5 and 18 weeks of gestation, and flash frozen in liquid nitrogen. Use of these specimens was deemed exempt from review by the institutional review board for human subjects at Northwestern University. Mouse prostate tissues were harvested from male BALB/c embryos at days 15 and 19 of gestation (20-day gestation period with day of the vaginal plug equal to day 0), and 5 and 10 days postnatally. Tissues were formalin fixed, paraffin embedded and serially sectioned. Adult C57BL/6J-$A^{w\text{-}J}$-Ta^{6J}+/+Ar^{Tfm} mice with mutant androgen receptors (testicular feminization [Tfm]) were used. Obtained from Jackson Laboratories.

Immunohistochemistry. Santa Cruz sc-1194 goat polyclonal antibody (Santa Cruz Biotechnology, Santa Cruz, California) (200 μg./ml.) to the *SHH* protein 19 kDa. amino terminus was used for immunostaining. *SHH* protein in human tissues was localized by indirect peroxidase staining. Representative sections were deparaffinized and hydrated. Endogenous peroxidase activity was blocked with 3% hydrogen peroxide in methanol for 10 minutes. Antigen retrieval was performed by microwave processing at full power for 15 minutes in 0.01 M. citrate buffer (pH 6.0). After overnight incubation with the primary antibody a rabbit anti-goat secondary antibody conjugated with horseradish peroxidase was applied. Slides were developed in a solution containing 3,3'-diaminobenzidine tetrahydrochloride and hydrogen peroxide. All sections were counterstained with hematoxylin. *Shh* protein was detected in developing mouse prostate by indirect alkaline phosphatase staining, as previously described.[8]

RNA isolation and reverse transcriptase-polymerase chain reaction (RT-PCR). Total RNA was isolated in Trizol (Invitrogen, from prostate tissue, as described previously.[10] RT-PCR reactions were performed, as previously described.[8] Briefly, 50 ng. total RNA were reverse transcribed and carried through 35 cycles of amplification using primers specific for human *SHH* or mouse *Shh* using an RT-PCR Core Kit (Applied Biosystems, Foster City, California). Semiquantitative RT-PCR assay of expression was performed as previously described using the ribosomal subunit gene RPL-19 as an internal control.[8] Reactions were routinely performed without RT to demonstrate the RNA dependence of reaction products. *SHH* yielded a 220 bp product, which was confirmed by restriction digestion with SmaI and NaeI. RPL-19 yielded a 544 bp product. RT-PCR primer sequences 5'–3' were *SHH* forward TCGGTGAAAGCAGAGAACTC, *SHH* reverse TCTCGATCACGTAGAAGACC, RPL-19 forward TCAGGCTTCAGAAGAGGCTC and RPL-19 reverse ATGATCTCCTCCTTCTTGGC. Primers for mouse *Shh* and RPL-19, and product sizes have been previously described.[8]

RESULTS

SHH localization in the fetal human prostate. Representative sections from 7 male fetuses at 9.5 to 34 weeks of gestation were stained with polyclonal anti-*SHH* antibody. At 9.5 weeks weak staining was seen in the epithelium of the prostatic portion of the urogenital sinus (fig. 1, *a*). There was little staining of a more cephalad section at the bladder neck (fig. 1, *b*). Regional specificity for urothelial *SHH* expression at this stage reflected similar regionalization of expression in the fetal mouse.[8] There was intense staining of all layers of the prostatic urothelium at 11.5 weeks, including areas of new budding where staining appeared particularly robust (fig. 1, *c* and *d*). *SHH* staining remained intense at 13 weeks (data not shown). At 16 weeks staining diminished slightly but there was still strong staining of the prostatic urethra, and noncannulated and cannulated ducts (fig. 2, *a* and *b*). Staining was generally diminished by 18 (data not shown), markedly diminished at 20 and absent at 34 weeks (fig. 2, *c* and *d*).

SHH expression was assayed in total RNA extracted from 2 freshly isolated human fetal prostate specimens at 15.5 and 18 weeks of gestation. Expression was observed at each time point (fig. 3). Lower intensity of the product band in the 18-week sample suggested lower expression at the later time point, reflecting immunostaining findings. However, verification by quantitative RT-PCR was precluded by extremely poor RNA yields from the tissue specimens (data not shown). Together our studies indicate that *SHH* expression in the human fetal prostate is up-regulated at the onset of ductal budding, most abundant during the early phase of prostate

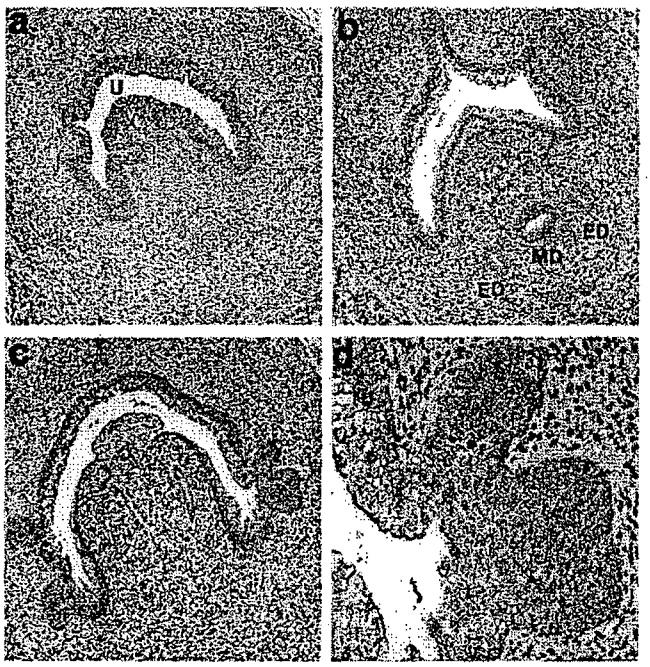

FIG. 1. Localization of *SHH* peptide in human fetal prostate by immunostaining. *a*, at 9.5 weeks of gestation there was weak staining of epithelium of urethra (*u*) in prostatic portion of urogenital sinus. Reduced from ×100. *b*, more cephalad section of urogenital sinus at bladder neck level near ejaculatory ducts (*ED*) and müllerian duct (*MD*) showed little staining. Reduced from ×100. *c*, at 11.5 weeks staining was seen in all prostatic layers. Reduced from ×100. *d*, at 11.5 weeks staining was noted in areas of new budding. Reduced from ×400.

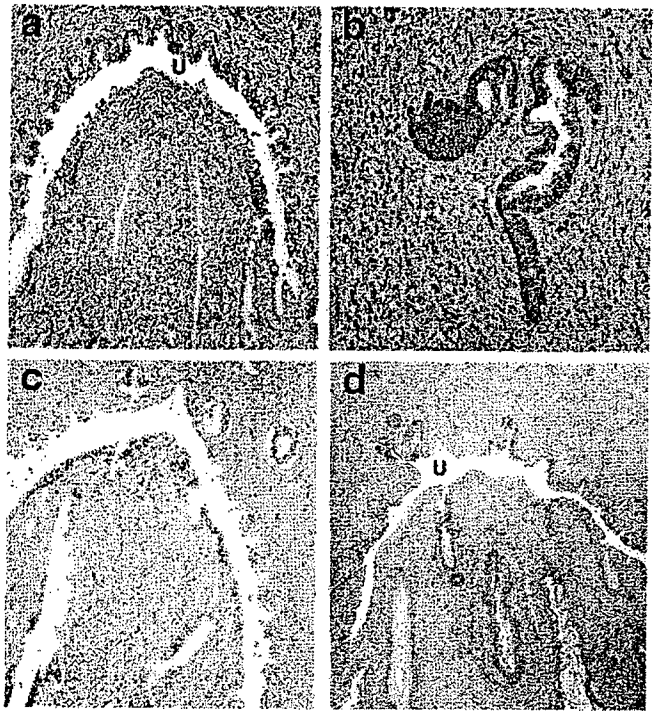

FIG. 2. *a*, at 16 weeks staining intensity in prostatic urethra (*u*) started to diminish. Reduced from ×100. *b*, noncannulated and cannulated buds remained intensely stained. Reduced from ×200. *c*, *SHH* staining was markedly diminished at 20 weeks. Reduced from ×100. *d*, *SHH* staining was essentially absent at 34 weeks. Reduced from ×40.

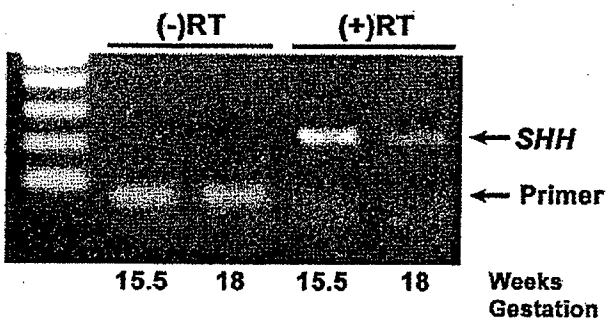

FIG. 3. *SHH* gene expression in human fetal prostate by RT-PCR at 15.5 and 18 weeks of gestation. Reaction product *SHH* was seen only by RT reactions. Diffuse bands at bottom of all lanes (*Primer*) represent unused primer sequences, which were more intense in negative (−) RT lanes, as expected. +, positive.

development, when ductal budding occurs, and down-regulated before birth.

To determine whether *SHH* expression in the urogenital sinus is unique to the male, immunostaining was performed in the human fetal female lower genitourinary tract. Staining was present in the urothelium of the urogenital sinus at 9 and 12 weeks (fig. 4). Staining was more intense in the section of the urogenital sinus above the entrance of the müllerian ducts. Staining was also seen in the wolffian duct. Staining diminished at 14 weeks and was almost absent at 18 (data not shown). These studies indicate that regionalized areas of *Shh* expression are present in the female lower genitourinary tract and also suggest that expression diminishes somewhat earlier in the female than in the male.

Shh expression in the developing mouse prostate. *Shh* expression in the developing mouse prostate is most abundant during late gestation (days 15 to 20) and the early postnatal

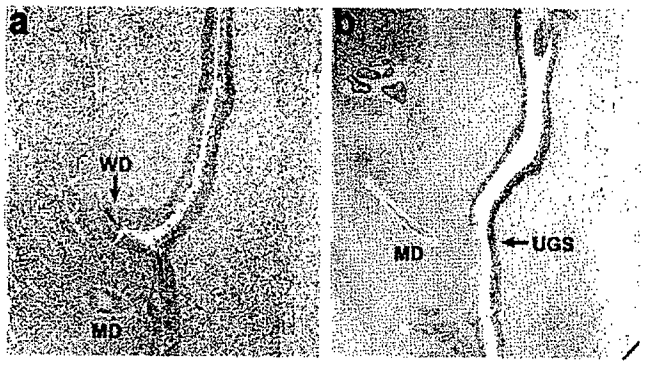

FIG. 4. Localization of *SHH* peptide in the lower urogenital tract of female fetus by immunostaining. Staining was localized to urogenital sinus (*UGS*) epithelium and was more intense cephalad to entrance of müllerian ducts (*MD*). Staining was also present in wolffian ducts (*WD*) but no staining was seen in müllerian ducts. *a*, at 9 weeks of gestation. Reduced from ×100. *b*, at 12 weeks of gestation. Reduced from ×40.

period (days 1 to 5), when most ductal buds are formed.[8] Immunostaining for *Shh* in sections of the urogenital sinus at day 15 of gestation showed diffuse staining of the prostatic urothelium (fig. 5, *a*). No staining of the mesenchyma was noted. After the onset of ductal budding at day 17.5 of gestation staining was seen at day 19 of gestation in the epithelium of the urethral lumen and nascent ductal buds (fig. 5, *b* and *c*). There was a similarity to immunostaining in the human fetal prostate at 11.5 weeks of gestation (fig. 1, *c* and *d*). Staining remained abundant at postnatal day 5 (data not shown) but it was generally diminished at postnatal day 10 (fig. 5, *d*).

We have previously shown that dihydrotestosterone stimulated *Shh* expression in the mouse urogenital sinus cultured in vitro.[8] The expression seen in the absence of dihydrotestosterone could indicate that *Shh* expression is not strictly androgen dependent. On the other hand, the urogenital sinus tissues used in these experiments were harvested after the onset of fetal testosterone expression at day 12 of gestation, leaving open the possibility that induction of *Shh* expression in the male as opposed to maintenance of expression is dependent on androgen. To exclude rigorously dependence of *Shh* expression in the male on testosterone we compared *Shh* expression in newborn Tfm male mice and their wild-type controls. Tfm is a frameshift mutation of the androgen receptor that renders males insensitive to androgens.[11] Assay for *Shh* expression by semiquantitative RT-PCR in the P1 urogenital sinus of male Tfm mice and their appropriate wild-type controls showed expression in each with apparently slightly lower expression in the mutant (fig. 6).

DISCUSSION

SHH expression in the human fetal prostate during ductal budding localized to the epithelial compartment. Most abundant expression was observed between 11.5 and 13 weeks, a period of extensive ductal budding, and diminished significantly at 18 to 20 weeks. This time course coincides with the fetal testosterone surge. Testosterone secretion from the testes begins at 8 weeks. Serum levels remain low (less than 100 ng/100 ml.) up to approximately 11 weeks.[12] Peak levels (100 to 580 ng/100 ml.) occur between 12 and 18 weeks, after which there is a sharp decline to low levels (less than 100 ng/ml.). The apparent correlation of *SHH* expression with the fetal testosterone surge should not be over interpreted. Testosterone stimulates *Shh* expression but the effect is modest.[8] These observations suggest that *SHH* expression is coordinated with the testosterone surge and may not necessarily reflect the direct dependence of expression on androgen.

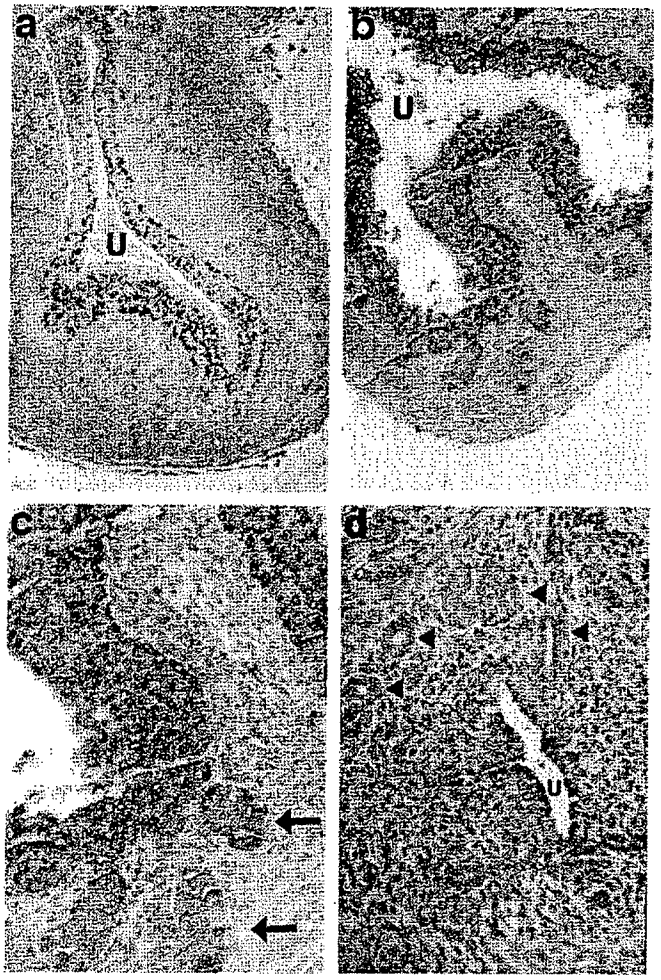

FIG. 5. Localization of *Shh* peptide in the fetal and neonatal mouse prostate by immunostaining. *a*, staining was present in urothelium of prostatic urethra (*u*) at day 15 of gestation. Reduced from ×200. *b*, staining at day 19 of gestation in prostatic urothelium. Reduced from ×200. *c*, staining at day 19 of gestation in nascent buds (arrows). Reduced from ×400. *d*, staining was significantly diminished at postnatal day 10, when there was slight staining of epithelium of urethral lumen but not in surrounding ducts (arrowheads). Reduced from ×400.

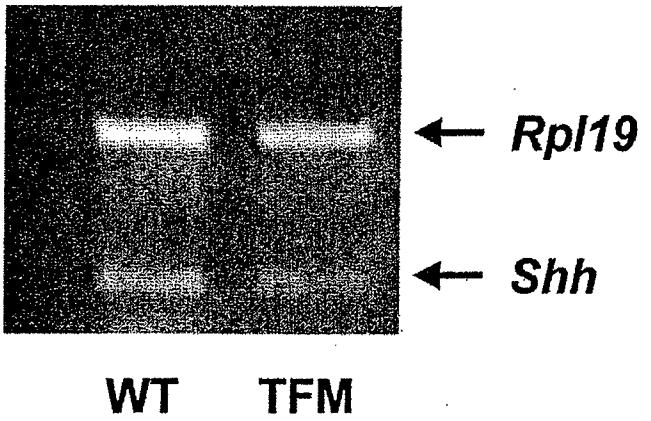

FIG. 6. *Shh* expression in P1 wild-type (*WT*) and Tfm (*TFM*) urogenital sinus by RT-PCR. Reactions performed using gene encoding ribosomal subunit RPL19 as internal control demonstrated *Shh* mRNA in each tissue. Control reactions performed without RT revealed RNA dependence of RPL19 and *Shh* reaction products (data not shown).

Prostate ductal budding absolutely depends on testosterone. In the absence of testosterone prostate ductal budding does not occur. Conversely budding can be induced in the female by exogenous testosterone. It may be interpreted as indicating that androgen functions as the switch to determine whether budding does or does not occur. Hedgehog signaling is also required for budding, as evidenced by the effect of antibody and chemical blockade of hedgehog signaling,[8,9] and *Shh* expression shows some degree of androgen regulation. However, *Shh* cannot substitute for testosterone since exogenous *Shh* does not stimulate glandular development in the male urogenital sinus grown as a subcapsular transplant in a castrated host.[8] Thus, prostate development requires testosterone and hedgehog signaling.

What is the action of *SHH*? *SHH* binding to its receptor on the target cell activates a signal transduction pathway that activates the transcription factor Gli1. Gli1 mediates hedgehog signaling by activating the transcription of *SHH* target genes by binding to Gli recognition sequences in the promoters. The closely related homologue Gli2 may provide functional redundancy in transcriptional activation, while another homologue, Gli3, may regulate the activities of Gli1 and Gli2.[5] Our studies of the developing mouse prostate indicate that hedgehog signaling up-regulates Gli1 expression in the urogenital sinus mesenchyma surrounding the developing buds.[9] Blockade of hedgehog signaling inhibits Gli1 expression in parallel with the abrogation of ductal budding.[9] This observation suggests that hedgehog signaling from the epithelium activates target gene expression in adjacent mesenchyma. Absent expression of the homeotic gene Nkx3.1 in the urogenital sinus of the *Shh* knockout mouse has been considered to suggest that Nkx3.1 is a target of hedgehog signaling.[13] *Shh* expression has been associated with up-regulation of Bmp4, Hoxd-13 and Fgf10 in the developing genital tubercle but it is thought that these effects likely involve connections with other regulatory cascades.[6] Further insight into the actions of *SHH* may come from identifying hedgehog target genes through microarray analysis.[7,14]

Outgrowth and extension of ductal buds in the developing mouse and human fetal prostate appear to result from concentrated epithelial proliferation.[15,16] As characterized in various experimental systems,[17,18] budding morphogenesis is process that usually involves an interplay of positive and negative growth regulators, which orchestrate a focal area of cell proliferation. This process produces a discrete site of epithelial outgrowth. While the hedgehog pathway and Gli family of genes (Gli1 to Gli3) appear to have a central role in prostate ductal budding,[8,9] a number of additional factors also appear to have a role. Mesenchymal FGF10 expression likely stimulates bud outgrowth and promotes ductal growth and branching.[19] Bmp4, which is also expressed in mesenchyma, acts as a negative growth regulator that may restrict budding to specific sites and inhibit epithelial proliferation between budding sites.[20] In the past it was anticipated that testosterone would be found to activate the expression of growth factors that stimulate ductal budding and branching morphogenesis but it does not appear to be the case. Thompson and Cunha reported that fibroblast growth factor-10 expression is similar in the male and female urogenital sinus.[19] Similarly Bmp-4 is expressed at equivalent levels in the male and female urogenital sinus, although the pattern of expression appears to be different in the 2 sexes.[20] These observations indicate that testosterone does not act simply as the upstream master switch, activating the expression of signaling activities in the urogenital sinus that produce prostate budding. They suggest a more subtle connection of androgen action with the activity of these signaling pathways. It may be a modification of the response to signaling, as suggested by Thompson and Cunha,[19] an effect on patterning the expression of these factors, as shown for Bmp-4,[20] or a combination of these 2 effects.

REFERENCES

1. Kellokumpu-Lehtinen, P.: The histochemical localization of acid phosphatase in human fetal urethral and prostatic epithelium. Invest Urol, **17:** 435, 1980
2. Aumüller, G., Groos, S., Renneberg, H., Konrad, L. and Aumüller, M.: Embryology and postnatal development of the prostate. In: Pathology of the Prostate. Edited by C. Foster and D. Bostwick. New York: W. B. Saunders Co., chapt. 1, pp. 1–17, 1990
3. Timms, B. G., Mohs, T. J. and Didio, L. J. A.: Ductal budding and branching patterns in the developing prostate. J Urol, **151:** 1427, 1994
4. Cunha, G. R., Sekkingstad, M. and Meloy, B. A.: Heterospecific induction of prostatic development in tissue recombinants prepared with mouse, rat, rabbit and human tissues. Differentiation, **24:** 174, 1983
5. Ingham, P. W. and McMahon, A. P.: Hedgehog signaling in animal development: paradigms and principles. Genes Dev, **15:** 3059, 2001
6. Haraguchi, R., Mo, R., Hui, C., Motoyama, J., Makino, S., Shiroishi, T. et al: Unique functions of Sonic hedgehog signaling during external genitalia development. Development, **128:** 4241, 2001
7. Yoon, J. W., Kita, Y., Frank, D., Majewski, R. R., Konicek, B. A., Nobrega, M. A. et al: Gene expression profiling leads to identification of GLI1 binding elements in target genes and a role for multiple downstream pathways in GLI1 induced cell transformation. J Biol Chem, **21:** 21, 2001
8. Podlasek, C. A., Barnett, D. H., Clemens, J. Q., Bak, P. M. and Bushman, W.: Prostate development requires Sonic hedgehog expressed by the urogenital sinus epithelium. Dev Biol, **209:** 28, 1999
9. Lamm, M. L. G., Catbagan, W. S., Laciak, R. J., Barnett, D. H., Hebner, C. M., Gaffield, W. et al: Sonic hedgehog activates Gli1 mesenchymal gene expression during prostate ductal bud formation. Unpublished data
10. Podlasek, C. A., Duboule, D. and Bushman, W.: Male accessory sex organ morphogenesis is altered by loss of function of Hoxd-13. Dev Dyn, **208:** 454, 1997
11. Charest, N. J., Zhou, Z. X., Lubahn, D. B., Olsen, K. L., Wilson, E. M. and French, F. S.: A frameshift mutation destabilizes androgen receptor messenger RNA in the Tfm mouse. Mol Endocrinol, **5:** 573, 1991
12. Reyes, F. I., Boroditsky, R. S., Winter, J. S. and Faiman, C.: Studies on human sexual development. II. Fetal and maternal serum gonadotropin and sex steroid concentrations. J Clin Endocrinol Metab, **38:** 612, 1974
13. Schneider, A., Brand, T., Zweigerdt, R. and Arnold, H.: Targeted disruption of the Nkx3.1 gene in mice results in morphogenetic defects of minor salivary glands: parallels to glandular duct morphogenesis in prostate. Mech Dev, **95:** 163, 2000
14. Kato, M., Seki, N., Sugano, S., Hashimoto, K., Masuho, Y., Muramatsu, M. et al: Identification of sonic hedgehog-responsive genes using cDNA microarray. Biochem Biophys Res Commun, **289:** 472, 2001
15. Sugimura, Y., Cunha, G. R., Donjacour, A. A., Bigsby, R. M. and Brody, J. R.: Whole-mount autoradiography study of DNA synthetic activity during postnatal development and androgen-induced regeneration in the mouse prostate. Biol Reprod, **34:** 985, 1986
16. Xue, Y., Sonke, G., Schoots, C., Schalken, J., Verhofstad, A., de la Rosette, J. et al: Proliferative activity and branching morphogenesis in the human prostate: a closer look at pre- and postnatal prostate growth. Prostate, **49:** 132, 2001
17. Jung, H. S., Francis-West, P. H., Widelitz, R. B., Jiang, T. X., Ting-Berreth, S., Tickle, C. et al: Local inhibitory action of BMPs and their relationships with activators in feather formation: implications for periodic patterning. Dev Biol, **196:** 11, 1998
18. Neubuser, A., Peters, H., Balling, R. and Martin, G. R.: Antagonistic interactions between FGF and BMP signaling pathways: a mechanism for positioning the sites of tooth formation. Cell, **90:** 247, 1997
19. Thomson, A. A. and Cunha, G. R.: Prostatic growth and development are regulated by FGF10. Development, **126:** 3693, 1999
20. Lamm, M. L., Podlasek, C. A., Barnett, D. H., Lee, J., Clemens, J. Q., Hebner, C. M. et al: Mesenchymal factor bone morphogenetic protein 4 restricts ductal budding and branching morphogenesis in the developing prostate. Dev Biol, **232:** 301, 2001